Advanced Materials Science and Technology Vol 4 Issue 2 2022
DOI: 10.37155/2717–526X–0402–1

REVIEW

Open Access

Omniscient Pte.Ltd.

Carbon Supported Catalysts in Fischer-Tropsch Synthesis: Structural Properties of Carbon Supports

Thaane Hlabathe, Joshua Gorimbo*, Mahluli Moyo and Xinying Liu

Institute for the Development of Energy for African Sustainability (IDEAS), Collage of Science, Engineering and Technology, University of South Africa (UNISA), Private Bag X6 Florida 1710, Johannesburg, South Africa.

***Correspondence to:** Joshua Gorimbo, Institute for the Development of Energy for African Sustainability (IDEAS), Collage of Science, Engineering and Technology, University of South Africa (UNISA), Private Bag X6 Florida 1710, Johannesburg, South Africa; Email: joshuagorimbo@gmail.com

Received: July 24, 2022; **Accepted:** September 15, 2022; **Published Online:** September 30, 2022

Citation: Hlabathe T, Gorimbo J, Moyo M and Liu X. Carbon Supported Catalysts in Fischer-Tropsch Synthesis: Structural Properties of Carbon Supports. *Advanced Materials Science and Technology*, 2022;4(2):047601. https://doi.org/10.37155/2717-526X-0402-1

Abstract: The structural properties of some carbon-based supports can prevent the formation of hot spots and improve catalyst stability at Fischer Tropsch Synthesis (FTS) temperature. Special attention and some examples are given to iron-based catalysts and their performance in FTS. The carbon supports' structural properties such as metal-support interaction, effect of particle size, the confinement effect, graphitization degree of graphene, and interrelationship of catalyst properties, are linked to their function in FTS for supported catalysts. The modification effects of the catalysts with functional groups, promoters and heat treatment are related to FTS performance. The potential research areas and challenges posed by carbon support structural properties' relationship to FTS performance are identified.

Keywords: Carbon support; Fe-catalysts; Fe-catalysts modification; Fischer-Tropsch synthesis; Hot spot formation

1. Introduction

The world has been facing problems relating to the production of clean energy over the past few centuries, and the twenty-first century is not immune to this problem[1]. In the twenty-first century the problem is worse, due to the rapid increase in population, which has led to a rise in energy demand[1]. This accelerated increase in population has resulted in energy demand problems and has caused a problem for the environment as pollution is rapidly increasing. Fossil and oil-derived fuels have been used as a major energy source since the last century. Reserves of these fuels are becoming depleted at such a rate that the world needs an alternative clean and environmentally friendly source of energy[2]. The

Fischer-Tropsch Synthesis (FTS) reaction is one of the most promising solutions to address this energy supply problem.

FTS is a catalytic-polymerization reaction that hydrogenates carbon monoxide to produce useful products such as paraffins, diesel oil, alkanes, alkenes and oxygenates[3]. Iron-based catalysts can be used in high-temperature FTS (300-330 °C) and have the advantage of suppressing the production of methane[2]. Iron is one of the most abundant metals on earth and the cheapest[4]. Researchers have performed studies on iron-based catalysts to ascertain the catalytic activity, selectivity and stability in FTS[3]. Supports, such as silica, titania and alumina, or carbon supports, have been used to allow maximum dispersion of the active phase, easy separation of the catalyst from the reaction products, and improved catalyst stability[5].

The disadvantages of strong metal-support interaction with silica, titania and alumina have been well-documented[5,6]. Reducing iron on these supports is a challenge because of the presence of mixed oxides, which increase the reduction temperature required[1,6]. Carbon supports have been shown to have weak metal-support interaction, which prevents the formation of mixed oxides[1,6,7]. Carbon supports are cheaper than conventional supports, are resistant to both acidic and basic media, are stable at a high temperatures, and can be prepared in a variety of macroscopic shapes[8].

The structural properties of carbon supports compared to conventional supports, such as high thermal conductivity and mechanical strength, are essential in high-temperature FTS reactions for catalyst stability. The high thermal conductivity and mechanical strength of some carbon supports like graphene and carbon nanotubes (CNTs) are important in the prevention of hot spots formation and catalyst decomposition[1]. The most common carbon supports in FTS include graphene, CNTs, carbon nanofibers (CNFs), carbon spheres (CSs), activated carbon (AC), and ordered mesoporous carbon (OMC). These supports have different shapes, which are very important for their applications. For instance, CNTs are tubular in shape, which is a very important feature for confining catalytic metals inside the support, allowing longer contact time and preventing sintering due to the high temperature. A similar phenomenon is also seen in ordered mesoporous carbon, which also confines catalytic species inside the porous channels.

Even though several reviews have been published on carbon supports dealing with their synthesis and properties[9] there is a lack of reviews relating to their structural properties with regard to performance in FTS[10-15]. In iron-based catalysts, properties such as the confinement effect, thermal conductivity and mechanical strength improve catalyst stability. Carbon supports such as graphene, CNTs and CNFs have high thermal conductivity, essential for suppressing hot spot formation and improving the catalysts' stability at a high temperature during FTS. The current review is structured as follows: The structural properties of carbon supports and their differences are discussed. The review relates structural and electronic properties of carbon supports such as metal-support interaction, iron phases, effect of particle size and the confinement effect, the degree of graphitization of graphene, as well as interrelationship of catalyst properties in FTS performance for iron-based catalysts. The modification effect of functional groups, promoters and heat treatments are also discussed. Finally, carbon foam that can be synthesized cheaply from agricultural waste, and which has excellent structural properties such as high thermal conductivity and mechanical strength, is brought to researchers' attention as a potential carbon support.

2. Structural Properties of Carbon Supports

Carbon materials' properties such as mechanical strength, thermal and electrical conductivity, the confinement effect, surface areas and porosity are necessary for differentiating carbon supports[16]. The carbon material properties are dependent on the method of synthesis, and these structural properties determine their applications[16]. This section looks at graphene, CNTs, CNFs, CSs, AC, CSs and OMCs structural properties.

2.1 Graphene

Graphene has a two-dimensional structure, developed porosity, a large active surface area, excellent electronic properties, and mechanical and thermal stability[17]. Graphene possesses a conjugated sp^2 hybridized planar structure, and this quality gives graphene high mechanical strength and ultra-high electrical and thermal conductivity[18]. It is an ideal thermal conductor showing ballistic and isotropic thermal conductance, and its thermal conductivity reaches values of 5000

W/(m·K) for a suspended single-layer graphene sheet at room temperature[19-21]. This value is greater than that of diamonds, graphite and CNTs. In terms of heat conductance, graphene can outperform most carbon materials such as CNTs[22].

Graphene has two different but equivalent carbon sublattices in the crystal structure that give graphene its unique electronic band structure and charge carriers' unusual behaviour. The structural defects of graphene are essential in catalysis, and it is easier to tailor the localized properties of graphene[23]. These lattice defects and functional groups help during graphene functionalization and in the anchoring of nanoparticles on graphene[18].

2.2 CNTs

CNTs are divided into single-walled carbon nanotubes (SWCNTs) and multi-walled carbon nanotubes (MWCNTs). The SWCNTs are made from graphene sheets that have hexagonal crystal structures as a result of sp^2 hybridized carbon atoms, rolled up into cylinders and closed by two caps. The MWCNTs are concentric with a larger diameter than SWCNTs. The MWCNTs can have double wall with an external diameter of up to 100 nm[8]. This material has no microporosity, which eliminates diffusion and interparticle mass transfer[17]. CNTs have high mechanical strength because of the C-C bonds and the geometrical structure. The C-C bond in the basal plane of graphite is known to be one of the strongest chemical bonds in nature.

The SWCNTs behave like quantum wires in that electrons are confined along the tube axis. In this material, the electronic properties are controlled by two factors - tube diameter and helicity - and this depends on the way graphene layers are rolled up. The curvature of graphene sheets in these materials introduces substantial modification of the electronic properties. The electronic properties of these materials are further modified by the presence of defects such as pentagons, heptagons, impurities and vacancies. On the other hand, MWCNTs electronic properties are like those of ultimate carbon fibres. The CNTs are known to be very conductive for phonons in the axial direction, whereas thermal conductivity is very low in the transverse direction. Theory predicts a high value for thermal conductivity for CNTs of 6000 W/(m·K)[8,17].

2.3 CNFs

There are three kinds of CNFs. Firstly, the herringbone in which the graphene layers are arranged obliquely with respect to the fiber axis. Secondly, the platelet in which the graphene layers are arranged perpendicular to the fiber axis. The way graphene sheets are aligned in CNFs determines the surface chemistry and reactivity[24]. The edges of CNFs are active for anchoring nanoparticles because of graphene sheets that have anchoring functional groups[24]. Thirdly, the ribbon. In this type, the graphene layers are arranged parallel to the growth axis.

The CNFs contain a conductive substrate that displays electronic properties like that of graphite. One study showed that CNFs have high mechanical strength with a tensile strength of 2.9 GPa and Youngs modulus of 240 Gpa[25]. The fibres have high electrical and thermal conductivity, and when heated to 3000 °C the thermal conductivity is four times that of copper[26].

2.4 CSs

CSs can be crystalline or semi-crystalline, with a solid, hollow or core shell morphology[11]. CSs have a low density and a high surface area, are thermally stable and have unique electronic properties. CSs are classified into three categories, based on the diameter: well-graphitized CSs with a diameter in the 2 nm to 20 nm range; less graphitized CSs with a diameter of 500 nm to 1000 nm; carbon beads with a diameter greater than 1000 nm[11]. The tensile strength of CSs have been measured by some researchers and were found to behave in a linear fashion[11]. CSs require no purifications to remove impurities from residual metal catalysts as in the case of CNTs and CNFs[27].

2.5 AC

The most important properties of AC are surface area, porosity, and pore size distribution[16,17]. The AC surface area depends on the raw materials used during synthesis and the degree and mode of activation[16]. The micropore volume of AC is reported to be up to 1.2 cm^3/g[8]. The AC has a larger surface area than conventional supports such as alumina and silica, and it is easy to control the porosity of AC. Still, most of the AC surface area is in the micropores, which are not accessible to the reactants. The AC porosity is responsible for the high adsorption capacity of these materials. Different researchers found AC thermal

conductivity values of 2.47 W/(m·K), 10 W/(m·K) and 30 W/(m·K)[28].

2.6 OMCs

Porous materials are divided into three classes: microporous with a pore size lesser than two nanometres (< 2 nm); mesoporous with a pore size of 2-50 nm; and macroporous > 50 nm[29]. OMC has been used as a support because of well-developed mesopores, thermal and chemical stability, high surface area and a conductive framework[24]. The OMC has a confining geometry of uniform nanometre sized mesopores in the range 2-10 nm[29]. This favours the formation of an active phase in the nanometre scale, which is excellent for catalysis[24]. The OMC denoted as CMK-3 has a hexagonal structure. It has a large surface area and pore volume because of mesoporosity generated after the removal of the silica template and microporosity[30]. The structure of OMC is affected by the nature of the carbon precursor and the conditions applied during the polymerization and the pyrolysis steps. It is advantageous to use OMC in catalysis because of large pores that facilitate mass transport and a very high surface area, allowing catalytic metals to be well dispersed[30]. The properties of carbon supports are summarised in **Table 1**.

Table 1. Summary of structural properties of various carbon supports

Supports	Diameter[a] (nm)	Apparent density (g/cm^3)	S_{BET} (m^2/g)	Porosity (cm^3/g)	Tensile strength (GPa)	Thermal conductivity[d] W/(m·K)	Ref.
SWCNTs	0.5-2 (1-1.5)	0.5-1	400-00	Microporous: V micro: 0.15-0.3	45-150	1000-6000[e]	[8]
MWCNTs	5-200 (10-40)	0.02-0.3[b]	150-450	Mesoporous: V meso: 0.5-2	3-30 to 150[c]	300-3000[b]	[8]
CNFs	10-500 (50-100)	0.3-1.4	10-250	Mesoporous: V meso: 0.2-2	3-30 to 150[c]	800-2000	[8]
OMCs	2-50	1.283	400-1000	Mesoporous: 0.7-3.8	0.042	10.34-14.50	[31-34]
CSs	2-1000 and above	0.16	2-1200	Microporous:	0.0378	1.7-15.9	[35-38]
AC	2-50 and above	2.0-2.1	500-2000	Microporous: 1.2	0.03	2.47, 10 and 30	[31,39-41]
Graphene	15.1	0.2-0.4	2630	Mesoporous: 1.28	130	5000	[19-21]

[a]: Typical values are in brackets; [b]: The lower value is powder; the upper value is for short MWCNTs; [c]: Defect-free MWCNTs; [d]: Axial thermal conductivity at room temperature (25 °C); [e]: A single rope of SWCNT

2.7 Synthesis of Carbon Supports

The synthesis and application of activated carbons have been investigated by different authors[42]. The synthesis can be from different carbonaceous materials[42]. For instance, the coal, agriculture by-products or lignocellulosic materials are the two main sources for the production of commercially activated carbons[43]. Among the applications of AC, it can be used as a support after synthesis and to further enhance its properties during catalysis, it is modified with promoters and treated with acids such as nitric acid to introduce nitrogen functional groups on the support.

The synthesis of CSs is like that of CNTs and CNFs. The CSs synthesis is performed using arc discharge, laser ablation, shock compression and chemical vapour deposition[11,44]. In the arc discharge technique, the discharge causes negative carbon electrode to sublimate at high temperatures and the carbon reconfigured as it cools and collected on the cathode in the reactor and the CSs are formed[44]. The laser ablation method uses a pulsed laser which vaporises a graphite target in a high temperature reactor and inert gas is blend into the reactor[44]. The carbon nanoparticles develop on the cooler surface of the reactor[44]. The shock compression method uses fullerenes as carbon source at high pressures to make CSs. Moreover, the chemical vapour deposition method is also used to synthesize CSs. This is where a volatile carbon source is converted into a solid non-volatile carbon product[44]. Cheng *et al*.[45] synthesized CSs using biomolecule dopamine containing carbon and nitrogen atoms as shown by **Figure 1**.

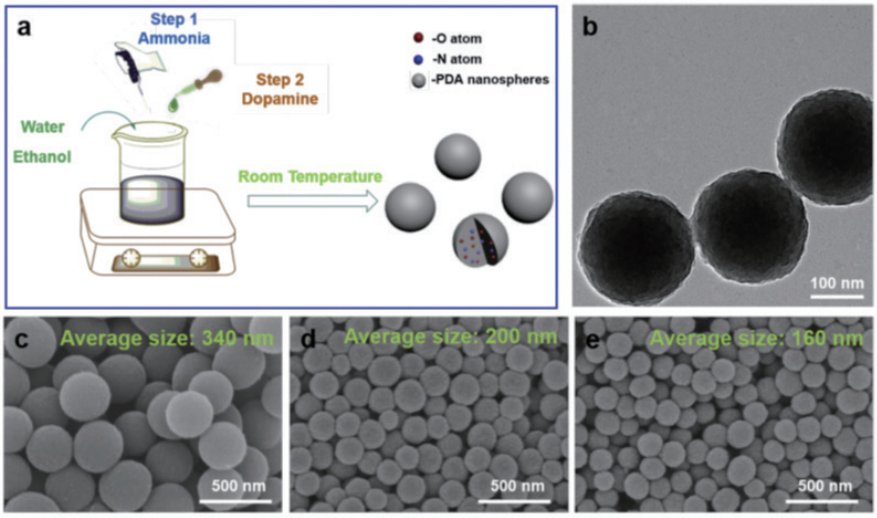

Figure 1. a) Illustration of the formation of nanospheres; b) TEM image of PDA nanospheres; c-e) SEM images of PDA nanospheres at molar ratio of ammonia to dopamine hydrochloride: c) 5.3, d) 8.0, e) 10.6. Adapted from ref. [45]

The CNTs are synthesized using laser ablation, chemical vapour deposition and arc discharge. In the laser ablation, the pulsed laser vaporises a graphite target containing a metal catalyst. In this method, the graphite target is placed in the furnace at the temperature of about 1200 °C in an inert atmosphere. The CNTs are deposited on the surface of the reactor as the vaporized carbon condenses. In chemical vapour deposition method, decomposition of hydrocarbons takes place in the presence of a particular transition metal catalyst for example Fe, Co, and Ni. The advantage of this method is that it is scalable to produce mass production of CNTs and is cheap. In the production of CNTs, the hydrocarbon vapour passes from a tubular reactor which have a high temperature furnace in the presence of a catalyst material at high temperatures of 600-1200 °C to decompose the hydrocarbons.

The arc discharge method is also used to synthesize CNTs. This method is the most common and the easiest. During the synthesis, two carbon rods are separated 1 nm to 2 mm in a closed environment filled with inert gases such as helium and argon at low pressures of 50 mbar and 700 mbar. Then a direct current of about 50 A to 100 A and 20 V are applied and this creates a high temperature of about 4000 K discharged between the two electrodes. The discharge vaporizes the rod in the anode and forms a small rod-shaped deposit on the rod in the cathode. **Figure 2** shows CNTs and CNFs synthesized with chemical vapour deposition method. The CNTs are modified with promoters and functional groups to enhance activity, selectivity, and stability of the catalysts during FTS.

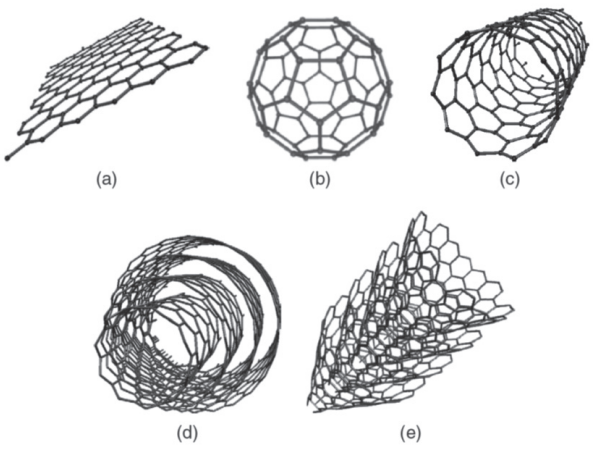

Figure 2. Representation of sp^2 carbon materials: a) graphite; b) C^{60}; c) single-walled carbon nanotube; d) multi-walled carbon nanotube; e) carbon nanofiber. Adapted from ref. [8]

The synthesis of graphene using chemical vapour deposition has been reported by many researchers. Reina reported the synthesis of few layer graphene on Ni films using chemical vapour deposition at the atmospheric pressure[31,46]. The same group induced precipitation of graphene on annealed polycrystalline Ni surface[46]. This method was used to produce a large single and bilayer graphene sheet where CH_4 was pyrolyzed at 1000 °C. Other researchers reported synthesis of few layers graphene using ZnS as a template by chemical vapour deposition. The decomposition of CH_4 at 700 °C on ZnS template and acid treatment to dissolve ZnS to produce graphene nanoribbons. The other alternative to produce graphene nanoribbons is by exfoliation of graphite. **Figure 3** shows a method used by Lee *et al*.[47] to synthesize iron carbide supported on graphene. This method uses melt infiltration sequence of hydrated iron salts and sequential thermal treatment under flow of carbon monoxide.

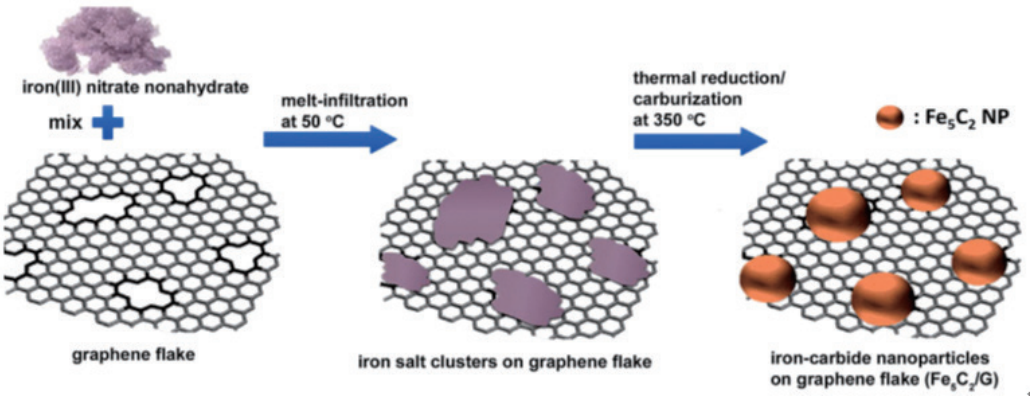

Figure 3. Synthesis of Fe_5C_2 on graphene flake catalyst. Adapted from ref. [47]

The synthesis of OMC is done by nano casting ordered mesoporous silica or zeolite templates or by templating triblock copolymer structure directing species[42]. In a typical synthesis of OMC, carbon precursor is infiltrated into the pores of ordered silica template, polymerized and then pyrolyzed in inert atmosphere to produce silica-carbon composite[42]. Then silica template is dissolved in HF leaving the desired material. The correct choice of silica template leads to tuneable pore sizes in the range of nanometers to micrometers and produce a three-dimensional ordered uniform structure having interconnected voids. For example, Liu *et al*.[48] the synthesized nitrogen functionalized mesoporous carbon using hard template assisted sol-gel polymerization method using phenol and formaldehyde as carbon precursors and melamine as nitrogen precursor as depicted by **Figure 4**.

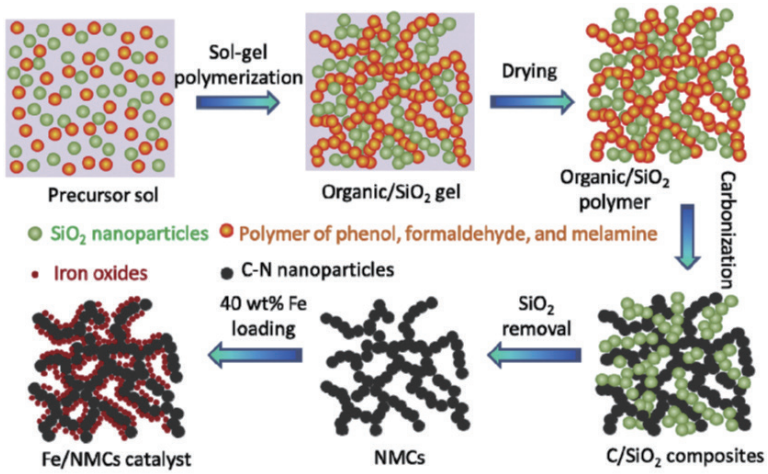

Figure 4. Scheme shows synthesize of nitrogen doped mesoporous carbon (NMCs) and iron metal supported on NMCs. Adapted from ref. [48]

The catalytic chemical vapour deposition is used to synthesize CNFs, as well as thermal and plasma methods are used to synthesize CNFs. In the catalytic chemical vapour deposition, the gas phase molecules are decomposed at high temperatures and carbon is deposited in the presence of transition metal catalysts on the substrate and then the growth of the fiber around the catalyst particle is realized. The process of catalytic chemical vapour deposition involves numerous stages such as gas deposition, carbon deposition, fiber growth and thickening as well as graphitization. The nanofiber diameter depends on the catalyst particle size. The catalytic chemical vapour deposition is divided into two categories which are fixed catalyst process (batch) and floating catalyst process (continuous). Tibbetts developed batch process, where they used mixture of hydrocarbon (CH_4), hydrogen and helium which was passed over crystalline aluminium silicate substrate with fine iron catalyst particles deposited at 1000 °C. They achieved fiber growth with several centimetres. In batch process method, the fiber length is controlled by gas residence time in the reactor. The continuous process method yields carbon fibers in the submicrometer diameters and few lengths of 100 μm and the definition of carbon nanofibers was derived from this method. During synthesis using continuous process method, organometallic compounds dissolved in solvent such as benzene yield a mixture of ultra-fine catalysts particles of 5-25 nm in diameter in hydrocarbon gas at temperatures of 1100 °C. The catalysts preparation can have a direct influence on the physicochemical properties of the catalysts. The FTS catalysts are usually prepared using wet impregnation, incipient wetness impregnation, coprecipitation and homogeneous deposition precipitation. Ghogia *et al*.[49] has reported on the preparation methods of carbon supports.

2.8 Iron Phases in FTS

The iron-based catalysts in FTS tend to show different iron phases under FTS reaction conditions. The iron phase changes have been reported by several authors to follow this order: Fe oxide (starting catalyst) →Fe metallic (reduced catalyst) → Fe carbide (active catalyst) [50]. The FTS reaction catalysts are in the form of iron oxide which are hematite (α-Fe_2O_3), maghemite (γ-Fe_2O_3) and magnetite (Fe_3O_4)[50]. The iron oxides are not active in forming hydrocarbons in FTS[51]. As a result of none activity of iron oxides, before FTS the iron oxides are reduced to metallic iron for example using gases like hydrogen or carbon monoxide. When this metallic iron is exposed to H_2/CO, during FTS reaction, the metallic iron reacts to form different iron carbides phases for instance, Fe_2C and Fe_3C[52]. Other authors can have decided to expose iron oxide to FTS reaction conditions for example H_2/CO. in this case, active iron carbides for FTS are formed along with iron oxide reduction to metallic iron[52]. During reduction of iron oxide with hydrogen temperatures $\geqslant$ 350 °C are used together with adequate time to reduce Fe_xO_y to metallic iron. The most stable form of iron carbide (θ-Fe_3C) decomposes around temperatures of 500-600 °C into metallic iron and carbon species. The most observed iron carbide during FTS reaction is Hägg carbide (χ-Fe_5C_2). The carbides are also seen as ε-$Fe_{22}C$, Fe_2C, ε-Fe_2C, ε-Fe_3C. The most observed iron carbides under FTS conditions are θ-Fe_3C (cementite) and Fe_7C_3 (Eckstörm-Adcock carbide) for further reading about iron carbides in Fischer-Tropsch synthesis, work by Paalanen and Weckhuysen can be consulted[52].

2.9 Structural and Electronic Properties of Carbon Supports

The shape and properties of carbon supports distinguish one from another. **Table 1** and **Figure 5** illustrate the properties and different shapes of carbon supports, respectively. The graphene, CNTs, and CNFs values for surface area, porosity, thermal conductivity and tensile strength are theoretical values. The thermal conductivity of OMCs, CSs and ACs are the experimental values from various studies as from **Table 1**. The CNTs are tubular or cylindrical in shape, which gives a choice of depositing catalytic metals on the interior or exterior of the tube. The advantage of depositing catalytic metals on the interior surfaces is that they are not as easily deactivated at a high temperature as the exterior of the CNTs. On the other hand, OMCs have ordered mesoporous channels. These ordered channels are a great advantage when the catalytic metals are located on the inside of the channels and, as with CNTs, they cannot be deactivated easily at a high temperature. The name CSs encompasses the different shapes of this support, which are an onion-like shape, microbeads, carbon balls and carbon nanospheres. The catalytic metals can be located inside CSs and in this case they are used as nano reactors. These supports function best

when catalytic metals are on the inside, as opposed to the outside.

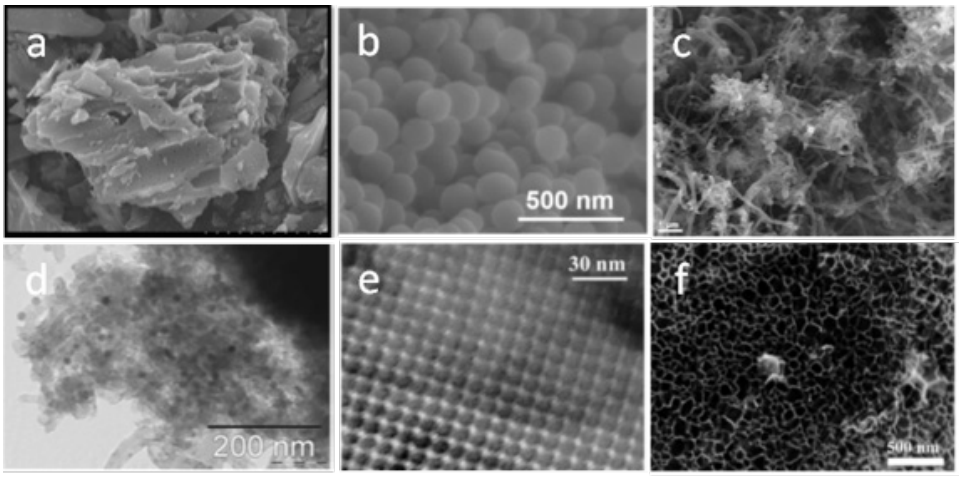

Figure 5. SEM images of: a) activated carbon[53]; b) carbon nanospheres (NCS-500)[45]; c) purified carbon nanotube[35]. TEM images of: d) carbon nanofibers[54]; e) ordered mesoporous carbon (CMK-1)[55]; f) graphene support[56]

The AC has a slit shape, so the location of metals is just on the surface. The CNF fibers are in a herringbone arrangement, or a platelet or ribbon shape (**Figure 5**). They also have catalytic metals on the surface of the fibers. the shape of graphene is sheet-like, so the catalytic metals are also found on the surface. These three supports, because of the location of the catalytic metal on the surface, can easily be deactivated at a high temperature.

It is not only the location of catalytic metals on the supports, which is crucial. Maximum surface area is also needed for catalysis. Surface area is important for maximum dispersion of catalytic metals to avoid agglomeration into larger particles that are deactivated quickly during the reaction. Looking at these carbon supports, graphene, AC and OMCs have larger surface areas than the other supports as illustrated in **Table 1**. It can be advantageous to use these supports where a larger surface area is required, but at moderate temperatures. The CNTs, CNFs and CSs have a minimum surface area as indicated in **Table 1**. Where a larger surface area is not a major priority for the catalysts, these supports can be used, and they have the advantage of the confinement effect.

The location of catalytic metals is dependent on the porosity of a support. The porosity of the support is crucial for its application. The same reactants can be used in a reaction but if the porosity of the support is changed, for instance, from microporous to mesoporous, different products will be obtained. The porosity of carbon supports is important for their application. **Table 1** shows that supports like AC and SWCNTs have micropores, which means they can be selective to certain products during the reaction, in comparison, the MWCNTs, OMCs and CNFs have mesopores.

CNFs have high mechanical strength and thermal conductivity. Among carbon supports, graphene is the most ordered followed by CNTs, CNFs, CSs, ACs and OMCs. This is because most of these carbon supports are made from graphene sheets. CNTs are graphene sheets rolled in a tubular form, and CSs are just graphene sheets in a spherical form. The high thermal conductivity and mechanical strength can prevent hot spot formation and catalyst decomposition, resulting in improved catalyst stability. The CNTs are tubular, and OMCs have channels, which means they can confine catalytic metals, while CSs are spherical. This means that they can be used as nanoreactors. The AC, graphene and OMCs have larger surface areas, which is good for the maximum dispersion of catalytic metals. The porosity of the support is important as it is selective to specific products.

The supported iron catalysts have gained interest due to their low rate of deactivation as compared to the unsupported iron catalysts[57]. The conventional supports such as titania, silica and alumina are known to have strong metal-support interaction which is unfavourable because the active species (iron carbide) are hindered by the support. To counteract this problem of strong metal-support interaction, carbon materials were introduced as supports in FTS. The carbon supports have high surface

area for metal dispersion, thermal and mechanical stability, and their surface properties are easily tailored and have weak metal-carbon interaction[57]. The weak metal-carbon interactions result in a facile reduction and formation of iron carbides phases. Moreover, carbon materials can be used both in acidic and basic solutions. The carbon materials have versatile surface chemistry which makes it easy to add functional groups on their surfaces and to vary their density by activation and post-treatments[2]. The carbon supports have oxygen containing groups on their surface which allows the tuning of support acidity, and this could affect the interaction between the support and iron species. The porous texture of carbon supports could lead to encapsulation of iron species inside of carbon support[2]. The confinement of iron inside carbon nanotubes modify the redox properties of encapsulated iron oxides and this enhances the activity of iron catalysts in FTS[58].

Carbon nanofibers are based on ordered parallel graphene layers arranged in a specific conformation. Carbon nanofibers are less prone to coke formation as compared with inorganic supports and in the case of deactivation it could be easy to recover active phase[59]. Carbon nanofibers have more defects in their structure which leads to high porosity as compared with carbon nanotubes[59]. Activated carbons have advantages such as resistance to acidic and basic media, stable at high temperatures in inert or reducing atmosphere, wide range of pore structures but the activated carbons have micro-porous structure which causes transport limitations to occur in the reaction[60]. On the other hand, carbon nanotubes have meso-porous structure which prevents the transport limitations which is observed in activated carbons. Graphene is a single layer material with unique electronic, thermal and mechanical properties and it has large specific surface area as well as high adsorption capacity. The moderate interaction of carbon supports, and iron can render high degree of reduction and carburization. The nanosheets like structure of graphene facilitates fast desorption of reaction intermediates[61].

Carbon spheres have curly graphitic flakes with sp^2 hybridization. Carbon spheres are considered as model supports because of nonporous and inert properties[62]. Porous supports such as mesoporous carbon are important for uniform active phase dispersion and to prevent severe agglomeration of active phase. Porous materials are good candidate for FTS because of high chemical stability and good thermal conductivity and weak metal-carbon interaction[63]. Porous carbons have enough contact time with active phase which facilitates the formation of iron carbides which is active phase in FTS hence high activities[36]. Carbon have a great advantage as outstanding reducing agent which can enable metal oxides to be reduced to metallic phases in the inert atmosphere what is termed as autoreduction[64]. The unique intrinsic properties and multifunctionality of metal/carbon have been shown to have important role in the formation of special products for FTS[65]. The carbon supports structural and electronic properties are linked to function in FTS for iron-based catalysts, as discussed in section 3.

3. How Structure Fits Function in FTS

Carbon in different forms and shapes has been applied as a support in FTS[66,67]. The performance of the various iron-carbon supported catalysts is strongly dependent on the structural properties of the carbon support used. Some of these carbon supports are derived from graphene, so they inherit high thermal and electrical conductivity from graphene sheets. This is important for removing excess heat from highly exothermic FTS reactions. The mechanical strength is almost the same as that of graphene. For this reason, they are very stable at high temperatures and under harsh reaction conditions. The structural properties that this review deals with are metal-support interaction, the confinement effect of CNTs and OMC, the degree of graphitization of graphene, surface area and porosity, as well as iron carbon-supported catalyst modification in FTS. The structural properties and modification of iron-based catalysts with functional groups, promoters, heat treatments and the impact on activity, selectivity and stability are reviewed in the following section.

3.1 Metal-support Interaction in FTS

Metal-support interaction is one of the significant factors that affect the FTS reaction in terms of activity, selectivity and catalyst stability[68]. Earlier works have shown that where silica, titania and alumina have been used as supports in FTS, they exhibit a strong metal-support interaction[20,68]. The strong metal-support interaction in these supports is seen with high reduction temperatures, which stem from mixed oxides. On the other hand, researchers have taken advantage of the weak metal-support interaction of carbon materials[20,68].

For example, in the study conducted by Karimi *et al*.[39], their supports which were graphene and carbon nanotubes for cobalt had a methane selectivity of 8.2% and 12.5% respectively. On the other hand, the study conducted by Abrokwah *et al*.[69], using 12% Ru/TiO_2 had a methane selectivity of 90% at 150 °C, as temperature was raised to 220 °C the methane selectivity decreased to 49%.

The carbon-based supports can lead to more olefin selectivity. The iron-based catalysts deposited on carbon based supports have been widely used for CO_2 hydrogenation due to its unique properties in hydrogen adsorption and spillover[70]. The catalyst prepared on carbon-based supports have influence on electronic properties. Carbon nanotubes are different from other carbon supports. Carbon nanotubes are graphene layers with tubular morphology. Some theoretical studies have revealed that deviation of graphene layers from planarity causes π- electron density to shift from the concave inner surface to the convex outer surface leading to an electron deficient interior surface and an electron enriched exterior surface[32]. This phenomenon can influence the structure and electronic properties of substances in contact with either surface[58]. Carbon based catalysts have advantage in terms of heat transfer of the reaction, for instance, large contact surface in nanosheets of graphene improve activity during FTS by providing a large surface density for reactants and decreasing mass transfer limitations[39].

The support that is required in FTS should have large surface area for metal dispersion, thermally and mechanically stable as FTS is performed at high temperatures for example at 220 °C and 20 bars so stability helps in terms of deactivation of the catalyst. The carbon supports are suitable for FTS reaction because are thermally stable, they are inert which makes easier to study the effect of other parameter on FTS such as particle size effect on activity and selectivity. In addition, carbon supports do not form mixed oxides as compared with conventional supports such as silicon oxide and titanium oxide. These mixed oxides make it difficult to reduce either cobalt or iron on the surface of conventional supports because of strong metal-support interaction.

3.1.1 Case studies in metal-support interaction

The metal-support interaction is affected by the nature of the support, the metal loaded and promoters[71]. Ma *et al*.[71] studied metal-support interaction on activated carbon using iron (Fe/AC) using a catalyst promoted with copper and potassium. They found that the addition of copper promotes the reduction of iron oxide to iron (FeO to Fe)[71]. In another study, Oschatz *et al*.[72] also studied the effect of sulphur and sodium as promoters for iron catalysts in relation to metal-support interaction[72]. They found that 15wt% and 30wt% sodium led to complete deactivation of the catalyst. This is because the high percentages of promoters block active sites and migration of the active phase on the surface of the support because of very weak metal-support interaction[72]. Kangvansura *et al*.[66] used Fe/NCNT promoted with potassium (K) and manganese (Mn). The unpromoted catalyst produced methane, compared to the K-promoted catalyst K/Fe/NCNT. The large production of methane was associated with strong metal-support interaction in unpromoted catalysts compared to the K-promoted catalysts that provided active iron for carbide formation, which is known to be highly active in FTS[66].

In another work, Ni *et al*.[73] used graphitic carbon (GC) to fabricate the $Fe@SiO_2$-GC core shell nanoparticles. The study results indicated strong interaction of dispersed FeO with Si-OH groups from SiO_2, as shown by the high reduction temperature of 522 °C. The reduction peak for FeO to Fe in one of the catalysts, $Fe@SiO_2$-GC-1, was 382 °C because of graphitic carbon modification that had weakened the interaction between FeO-SiO_2 and also decreased Fe and Si-OH interaction, which in turn promoted the reduction of FeO to Fe[73]. **Table 2** summarizes the reduction temperatures from different studies. The reduction temperatures on the supports are strongly linked to metal-support interaction. For example, the higher the temperature the stronger the metal interaction with the support.

Table 2. Various carbon supports and the reduction temperature, as per various authors

Support	Reduction temperature (°C)		Ref.
	Fe_3O_4 to FeO	FeO to Fe	
Graphene	-	382	[73]
CNTs	411	567	[58]
CNFs	688	783	[59]
CSs	331	501	[40]
ACs	410	470	[4]
OMCs	360	603	[48]

The metal-support interaction is affected by certain factors such as the preparation method for the catalyst and the functionalization of the support with functional groups such as nitrogen and oxygen. These can introduce defects in the support which affect the formation of iron carbide by either increasing or decreasing the reduction temperature. The promoters also affect the metal-support interaction, which also affects the formation of iron carbide during reduction.

Wei *et al*.[41] used thermal pre-treatment in argon to reduce the strong interaction between graphene oxide and iron oxide. They found that the reduction peak for the catalyst Fe/GO-500 was shifted to lower temperatures, confirming weak interaction between GO and iron oxide[41]. The same group of Wei *et al*.[74] went further to study the interaction of graphene oxide with iron oxide using the hydrothermal method with three different iron precursors: ferrous acetate $Fe_2(C_2H_3O_2)_2$ denoted as Fe/G-A; ferric oxalate $Fe_2(C_2O_4)_3$ denoted as Fe/G-C; ferric nitrate $Fe(NO_3)_3$ denoted as Fe/G-N. The catalyst Fe/G-C had a weaker Fe-GO interaction, which promoted reduction and carburization.

Xiong *et al*.[75] used iron supported on CSs in FTS. They prepared iron supported on functionalized CSs using impregnation and incipient wetness impregnation. They observed that the addition of K as a promoter decreased catalytic activity, but increased olefin selectivity. They found that the addition of Cu improved iron reduction and suppressed gasification on CSs support. The good performance of the catalysts was attributed to reduced metal-support interaction compared to oxide supports[75].

The carbon materials have weak metal-support interaction with catalytic metals. The large percentages of promoters affect metal-support interaction negatively as iron particles bond strongly to the support, which reduces the number of active sites. The graphitic carbon can also be used as a modification to tune metal-support interaction.

3.2 Effect of Particle Size in FTS

The effect of particle size of cobalt or iron on FTS have been studied by several author[54,76]. Furthermore, Bezemer *et al*.[77] performed a study to determine the effect of cobalt particle size on the activity on Fischer-Tropsch synthesis and carbon nanofiber was used as a support. In this study cobalt particle size in the range of 2.6-27 nm were used to correlate their effect on activity and selectivity. They found that as cobalt particle size decreased from 16 nm to 2.6 nm, the C_5^+ selectivity also decreased from 85% to 51%[77]. In addition, Hirsa *et al*.[54] studied iron particle size effect on the production of lower olefins from synthesis gas. The study was on the effect of iron carbide particle size on promoted and unpromoted catalyst supported on carbon nanofibers. They performed FTS at reaction conditions of 340-350 °C, $H_2/CO = 1$ and pressure of 1 and 20 bars. They found that the initial activity of unpromoted catalysts at 1 bar increased 6-8 folds when particle size of iron carbide decreased from 7 nm to 2 nm and the selectivity of lower olefins as well as methane were not affected[54]. On the other hand, as particle size decrease from 7 nm to 2 nm for catalysts promoted with Na and S at 20 bars, they noticed a 2-fold increase on TOF based on the initial activity and this was caused by a higher yield of methane for the smallest particle size[54]. The effect of particle size in FTS is of paramount importance, in other studies like the one conducted by Bezemer *et al*.[77] as cobalt particle size decrease from 16 nm to 2.6 nm C_5^+ selectivity also decreased while on the study conducted by Hirsa *et al*.[54] as iron carbide particle size decreased from 7 nm to 2 nm, they have seen an increase of 6-8 folds of lower olefins. Therefore, there is still some controversy on the effect of particle size on FTS hence more studies are still required on this issue.

3.3 Confinement Effect in FTS

Among the carbon supports used in FTS (graphene, CNTs, CNFs, CSs, AC, CNFs and OMCs), only CNTs and OMCs have a confining ability due to the structure[33]. CNTs are tubular, allowing the catalytic metals to be deposited on the inside or outside of the tube. The deposition of catalytic metals on the inside of CNTs provides enough contact time between the catalysts and the reactants (syngas), resulting in improved activity and selectivity[33]. In addition, when catalytic metals are located on the inside of CNTs they are not easily deactivated compared to when they are located outside the CNTs[33].

3.3.1 Confinement effect of CNTs in FTS

Carbon nanotubes have unique properties such as uniform pore size distribution, meso and macro pore structure, inert surface properties and resistance to acid[33]. Carbon nanotubes are tubular in shape therefore

this can allow catalytic species to be deposited on the inside or outside of carbon nanotube, when the catalytic species are on the inside of carbon nanotubes it is termed as confinement effect[58]. The confinement effect is important by allowing the reactant to have longer contact time with catalytic species and it is also useful in improving the stability of the catalyst by preventing easy migration of catalytic species[33].

Researchers have studied the impact of the confinement effect using CNTs as a support for iron-based catalysts[34]. Chen *et al*.[34] studied how the confinement of the catalytically active components within CNTs affect the catalytic performance in FTS. They found that the reducibility of the confined catalyst was remarkably improved in either H_2 or CO[34]. They observed a substantial increase in the yield of C_5^+ hydrocarbons with confined iron, which was twice that of the iron on the outside of CNTs[34]. This is because trapping the intermediates inside CNT channels prolongs the contact time with the iron catalyst, which favours the growth of longer chain hydrocarbons[33]. Casavola *et al*.[37] used iron as a catalyst. The catalyst Fe/CNT-T-350 catalyst had 59% selectivity towards C_2-C_4 olefins. The good performance of the catalyst in terms of stability was attributed to the ability of CNTs support to confine iron nanoparticles inside the tubes[33,38]. Lama *et al*.[21] reported synthesis of Fe/NCNTs and used sodium and sulphur as promoters. The catalyst was stable during time on stream because of the confinement effect of CNTs[68,78].

Other researchers embedded iron carbide into hollow CSs to improve the stability at a high temperature[79]. The TEM images showed that the catalyst possesses a well-defined hollow sphere morphology with embedded Fe particles. They reported improved selectivity of C_2-C_4 olefins and C_5^+ hydrocarbons. This was because of the hollow structure of CSs ,which allowed good dispersion, robustness and resistance to sintering[79].

Abbaslou *et al*.[58] developed a method to manipulate the catalytic site positions on the interior or exterior surface of the CNTs. The catalysts used were denoted in-Fe/CNT and out-Fe/CNT to distinguish their position on the CNT. The results from TEM confirmed that 70%-80% of the iron oxide particles were controlled to be deposited on the interior of CNTs. Both catalysts in-Fe/CNT and out-Fe/CNT had a CO conversion of approximately 90% (**Figure 6**). The out-Fe/CNT catalyst experienced deactivation within a period of 125 h on stream because of sintering due to lack of the confinement effect compared to the in-Fe/CNT catalyst[58].

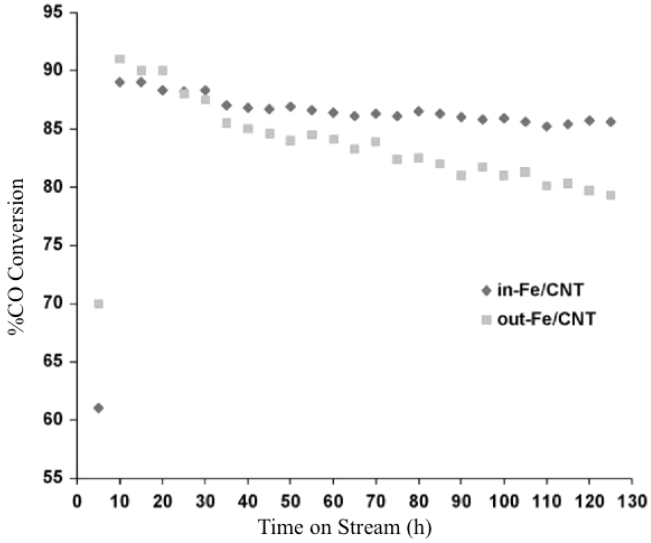

Figure 6. Change in % CO conversion with time on-stream for in-Fe/CNT and out-Fe/CNT catalysts. (Process conditions: 2 Sl/g-cat/h, P = 2 MPa, H_2/CO = 2, T = 270 °C, TOS of 125 h). Reproduced with permission from ref. [58]

3.3.2 Surface reaction on CNTs

The reaction on CNTs can take place on the interior or exterior of the CNTs. The immobilization of metals on the exterior and interior surfaces of CNTs have an impact on the FTS in terms of selectivity and activity. Other researchers have compared the activity and selectivity on CNTs interior and exterior surfaces. Chen *et al*.[34] compared the interior and exterior of CNTs

and AC in terms of activity and selectivity in FTS. They prepared three catalysts, denoted Fe-in-CNT, Fe-out-CNT and Fe/AC. The results of the study are summarized in **Table 3**.

Table 3. Catalyst location in the support and their performance in FTS[78]

Carbon support	Performance			Hydrocarbon (selectivity %)		
Catalysts	CO conversion (%)	Yield (g C_5^+/Kg_{cat}.h)	CO_2 selectivity (%)	CH_4	C_2-C_4	C_5^+
Fe-in-CNTs	40	440	18	12	41	29
Fe-out-CNTs	29	210	12	15	54	19
Fe/AC	17	61	5	15	71	9

Yang *et al*.[80] prepared FeN nanoparticles supported on CNTs for FTS. The catalysts used were denoted F_xN-in-500 and F_xN-out-500. These catalysts were nitridated at 500 °C, and it was found that the confined FeN was more active than the FeN on the outside of CNTs. The F_xN-in-500 catalyst had 22.9% selectivity for C_5^+ compared to the F_xN-out-500 catalyst that had 20.9%. Xiong *et al*.[57] prepared an iron catalyst supported on nitrogen-doped CNTs. The purified CNTs had a surface area of 91 m^2/g and pore volume of 0.34 cm^3/g, while the N-CNT-700 catalyst had a surface area of 85 m^2/g and a pore volume of 0.30 cm^3/g. The Fe/CNT-m catalyst had a C_1 selectivity of 30% and the Fe/N-CNT-m catalyst had a C_1 selectivity of 63.5%.

3.3.3 Confinement effect of OMCs in FTS

The inorganic substrates give catalysts stability by preventing particle growth and mechanical breakdown[81]. Moreover, the chemical properties, pore size, pore geometry and pore connectivity have a significant impact on the size and dispersion of catalytic metals[27]. Ordered mesoporous substrates come in different varieties such as ordered mesoporous silica (SBA-15), ordered mesoporous carbon (CMK-3) and ordered mesoporous silicon carbide (OM-SiC)[64,82]. Ordered mesoporous substrates are important because of their long-range ordered pore structure with a high geometry and narrow pore size distribution[36]. In addition, the stability of catalysts is increased by the encapsulation nature of ordered mesopores system compared to support with large and disordered mesopores[36].

The confining ability of OMC during FTS has been demonstrated by other researchers[48,82]. Oschatz *et al*.[83] used CMK-3 with different nitrogen functional groups as support for Fe based catalysts and sodium and sulphur as promoters in FTO. The oxygen functional groups were found to bind strongly to the confined Fe particles during calcination and this blocked iron active sites. The promoters gave 3 to 5 times higher activity[83]. CMK-3 confined the Fe nanoparticles, but did not prevent particle growth, which led to a decrease in catalytic activity under FTO conditions[83,84]. In addition, the effect of SBA-15, CMK-3 and OM-SiC and that of sodium and sulphur promoters was studied by Oschatz *et al*.[85] using FTO as a model reaction. They ascribed excellent stability and selectivity of CMK-3 to the confining channels of CMK-3[65,85].

Sun *et al*.[29] synthesized CMK-3 support with uniform metal containing nanoparticles using a chelate assisted multicomponent co-assembly method. The TEM images of the results showed that the nanocomposite of the Fe-C-z samples had a stripe-like, hexagonally arranged pore morphology, which is associated with an ordered mesostructure with a two-dimensional pore symmetry. The catalyst Fe-C-8 had C_5^+ selectivity of 68% and CH_4 selectivity of 8.2%[29]. They took advantage of the semi-exposed structure of CMK-3 where iron nanoparticles were partially embedded in the carbon framework and the remaining part exposed in the mesopore channels[29]. This unique structure provided excellent confinement and also exposed catalytic sites for catalysis[29].

The confinement effect of CNTs and OMC supports is important in the stability of iron-based catalysts at a high temperature. Iron nanoparticles on the outside of the tubes of CNTs and out of the channels of OMC are likely to be deactivated. In some cases, the confinement effect of CMK-3 did not prevent particle growth, which led to lower activity.

3.4 Graphene Graphitisation in FTS

An important property of graphene is that it can be graphitized compared to other carbon supports due to its sheet like shape[47,73,86]. It is easy to orientate fibers in graphene in the same direction compared to AC, CNTs, CNFs, OMC or CSs. Graphene can undergo different

kinds of defects that can change its structure and physicochemical properties[87]. The defects can change the topology or curvature of graphene[87]. In addition, the defects on graphene change its chemical activity[87]. Promoters increase defects on graphene, which modify its surface chemistry[56]. Raman spectroscopy is used to determine the defects on carbon materials such as graphene. The G band originates from sp^2 hybridized carbon atoms and the D band arises from structural disorder due to defects on graphene[56]. The ratio of D band to G band (I_D/I_G) is a measure of the disorder in carbon materials that is linked to the degree of graphitization. The degree of graphitization of graphene depends on the degree to which the fibers that make up the graphene layers are aligned. The thermal and electrical conductivity of graphene depends on the degree of graphitization, which in turn affects the performance of the graphene support in applications such as in FTS.

The ratio of the D and G bands has been used by some researchers to investigate the defects in their prepared catalysts[56]. Cheng *et al*.[56] fabricated a 3D honeycomb like structured graphene (HSG) supported potassium promoted magnesium ferrite catalyst for FTS. The HSG showed Raman peaks at 1346 cm^{-1} for D band and at 1584 cm-1 for G band. The ratio of I_D/I_G was 1.08, which indicates that HSG was highly defective. Cheng *et al*.[88] studied the effect of potassium in reduced graphene oxide supported iron catalysts for FTO. The catalysts FeK2/rGO and Fe/rGO showed bands at 1345 cm^{-1} for the D band and 1585 cm^{-1} for the G band. The I_D/I_G ratio of both catalysts, Fe/rGO and FeK2/rGO, was found to be 1.26. This study correlated well with the previous study performed by the same group[56] in terms of the importance of defects on graphene. The defects acted as nucleation sites to anchor the active phase.

In another study, Tian *et al*.[89] synthesized an iron carbide catalyst encapsulated in graphene by pyrolysis of an iron glucose precursor. The catalyst was promoted with potassium (0wt% 5wt%). The Raman spectroscopy of the catalyst 2wt% K-Fe_3C@C showed a peak at 1350 cm-1 for D band and a peak at 1580 cm^{-1} for G band. The I_D/I_G ratio of catalyst 2wt% K-Fe_3C@C was 0.99, which indicated that the catalyst was well graphitized. The addition of potassium increased defects on graphene layers and facilitated the formation of iron carbides[89]. These results are in agreement with the study carried out by Moussa *et al*.[90], who synthesized a catalyst promoted with potassium. The authors explained the high activity and selectivity of the catalyst as being a result of defects within the graphene lattice, which acted as nucleation sites to anchor the iron nanoparticles[39,47].

Graphene is a single layer material, which possesses unique optical, electronic, thermal as well as mechanical strength properties[39]. In another study, the group of Karimi *et al*.[39] performed a study where they were comparing the activity of 15wt% cobalt prepared with wet impregnation supported on graphene as well as in carbon nanotubes. It is well known that mass transfer limitations and cobalt dispersion play a crucial role in the rate of catalytic reaction and in the rate of conversion as well as product formation[39]. Cobalt supported on graphene was found to have particle size of 4.3 nm as compared with on carbon nanotube with particle size of 4.8 nm. The two catalysts had percentage reduction of 72% and 64% respectively. The average cobalt particle size decreases on graphene due to high surface area and lower degree of agglomeration[39]. Besides particle size, different supports have different internal mass transfer limitations based on their structures. Graphene based catalysts are highly active, very stable in harsh conditions (for instance, in high temperatures because of thermal and mechanical properties.) The structure of graphene is unique as it is nanosheets and almost has no limitations of internal mass transfer for the reaction hence excellent FTS results are obtained. In addition, the large contact surface in nanosheets of graphene also improve the activity during FTS by providing a large surface density for reactants and decreasing mass transfer limitations[39]. In the case of carbon nanotubes, it has been found that the deposition of cobalt nanoparticles on the outer of CNTs facilitates reactants diffusion but there are mass transfer limitations in the inner surface[39]. At the reaction conditions of 220 °C, 1.8 Mpa, H_2/CO = 2 and 0.6 g catalysts, Co/graphene had 88.75% of C_5^+ and Co/CNTs had 84.16% of C_5^+ and CH_4 was found to be 8.2% and 12.5% respectively[39].

In summary, the defects on graphene act as nucleation sites that facilitate anchoring of iron nanoparticles; this prevents migration of iron nanoparticles from the graphene support, resulting

in high stability of graphene-based catalysts with excellent activity and selectivity. Graphene has no internal mass transfer limitations during reaction, and this enhances selectivity and activity in FTS.

3.5 Interrelationship of Catalysts Properties in FTS

The performance of the catalyst in FTS is influenced by several factors such as particle size, structural and electronic properties, surface area and porosity[16,91]. The catalyst can have large surface area for metal dispersion and large volume for accommodating large amounts of metal loadings. If the active species poorly interact with the support, the migration of active species will be seen regardless of large surface area and porosity or if metal-support interaction is strong the active phase will be hindered from catalysis which leads to poor activities and selectivities in FTS. Therefore, the well-designed catalyst should have large surface area, large pore volume and excellent structural and electronic properties as these factors are highly interwoven for good performance of the catalyst in FTS.

Table 4 summarises the information regarding the types of carbon supports, the preparation methods, the reaction conditions, the BET surface properties and the products obtained during FTS using iron as the active phase. As can be seen in **Table 4 (entries 2 and 5**), the AC support has a larger surface area (1170 m^2/g) than other supports, such as CSs (**entries 6 and 7**), CNTs (**entries 15 and 16**), OMCs (**entries 11 and 12**) and the graphene support (**entry 10**). The pore volume of the OMCs (**entry 11**) is the largest with 0.86 cm^3/g compared to the other entries. These studies support the statements made in section 2 where the structural properties of different carbon supports were discussed. Looking at the FTS performance of these supports, the CO conversion ranges from 24% (**entry 7**) for CSs to 98% (**entry 5**) from AC support. The AC support has the largest CO conversion (%) and the largest surface area. Using C_5^+ product as an example from the entries discussed, the C_5^+ selectivity ranges from 53.7% from AC (**entry 1**) to 80% from CSs (**entry 7**). The C_5^+ selectivity did not depend on a large surface area, as CSs with a surface area of 411 m^2/g had the highest C_5^+ selectivity. This shows that the structural and electronic properties of the support are very crucial. carbon spheres are made from curly graphene layers so they can be very stable at high temperatures as compared with activated carbons because of high thermal conductivity and mechanical strength as well as CSs act as nanoreactors during the FTS reaction which prevented migration of active species.

Table 4. Summary - carbon supports, preparation, reaction conditions, catalysts properties and FTS results, as per various authors

Entry	Catalyst	Preparation method	Conditions	Reactor	Surface area (m^2/g)	Ore volume (cm^3/g)	Ore size distribution (nm)	Particle size (nm)	Results	Ref.
1	Fe/AC	IWI	Temp = 300 °C P = 20 bar H_2/CO = 2.1 GHSV = 16 $Lh^{-1}g^{-1}$	Fixed bed	558	0.4	--	--	XCO = 64.0% iron time yield = 88.4 C_5^+ = 53.7% C_2^o-C_4^o = 21.2% C_2^p-C_4^p = 17.3% O/P = 1.2, CH_4 = 7.8% CO_2 = 34.1%	[2]
2	Fe/CQ	IWI	Temperature = 240 °C Pressure = 20 bar CO/H_2 = 1:1 GHSV = 16 NL $g^{-1}h^{-1}$	Stainless steel fixed bed	255	0.735	--	3±0.1	XCO = 14% C_5^+ = 74% C_2-C_4 = 18% CH_4 = 4% CO_2 = 4% α = 0.742	[92]
3	FeK/CQ	IWI	As above	As above	230	0.75	--	7±0.2	XCO = 18.8% C_5^+ = 78.1% C_2-C_4 = 12% CH_4 = 4% α = 0.763	[92]

Continuation Table

Entry	Catalyst	Preparation method	Conditions	Reactor	Surface area (m^2/g)	Ore volume (cm^3/g)	Ore size distribution (nm)	Particle size (nm)	Results	Ref.
4	K/Fe/CQ	IWI	As above	As above	240	0.78	--	5.3±0.1	XCO = 11.1% C_5^+ = 93% C_2-C_4 = 1.7% CH_4 = 2.2% α = 0.840	[92]
5	Fe-Cu-Mn/AC	Co-precipitation	Temperature = 300 °C Pressure = 20 bar H_2/CO = 4 GHSV= 2.0 $ghmol^{-1}$	Fixed bed	1170	--	--	--	XCO = 98% Yield = 34% C_2-C_6 = 42% STY = 232 mg gh^{-1}	[53]
6	10Fe/CS	As above	As above	As above	402	0.22	2.8	12.9	XCO = 25% C_5^+ = 70% C_1 = 18% C_2-C_4 = 12% CO_2 = 9%	[40]
7	5Fe-5Co/CS	Deposition co-precipitation	As above	As above	411	0.24	2.4	14.4	XCO = 24% C_5^+ = 80% C_1 = 11% C_2-C_4 = 9%	[40]
8	Fe_5C_2@C/NPC	Solid state	Temperature = 340 °C Pressure = 15 bar H_2/CO = 1	Fixed bed stainless steel	400	0.31	--	17.2	XCO = 96.4% FTY activity = 4.3×10^{-4} mol $g^{-1}s^{-1}$ C_5-C_{12} = 33.5% α = 0.8183	[93]
9	Fe_3@C/NPC	As above	As above	As above	336.4	0.26	--	--	FTY activity = 4.1×10^{-4} mol g^{-1} s^{-1}	[93]
10	Fe_5C_2/G	IWI	Temperature = 340 °C Pressure = 15 bar H_2/CO = 1.0 GHSV = 72 $NLg^{-1}h^{-1}$	Fixed bed	193	0.25	3-4	14	XCO = 91.8% FTY activity = 6.5×10^{-4} $molg^{-1}s^{-1}$ C_5^+ = 4.41 g $g^{-1}h^{-1}$ α = 0.832	[47]
11	40FeK/SMC	IWI	Temperature = 260 °C Pressure = 10 bar H_2/CO = 1	Fixed bed	356	0.86	9.7	--	XCO = 78.2% TOF = $1.52\times10^{-3}s^{-1}$ C_5^+ = 61.0% C_2-C_4 = 22.9% CH_4 = 7.8% CO_2 = 47.1%	[36]
12	Fe/PMC1	IWI	Temperature = 513-543 K Pressure = 20-30 bar CO/H_2 = 1:1	Slurry	147	0.23	2.4	--	XCO = 40% C_1-C_4 = 47.3% C_5-C_9 = 35.8% C_{10}^+ = 16.9%	[30]
13	Fe/PMC2	As above	As above	As above	34	0.11	1.7	--	XCO = 45% C_1-C_2 = 20.8% C_5-C_9 = 70.3% C_{10}^+ = 8.9%	[30]

Continuation Table

Entry	Catalyst	Preparation method	Conditions	Reactor	Surface area (m^2/g)	Ore volume (cm^3/g)	Ore size distribution (nm)	Particle size (nm)	Results	Ref.
14	Fe/CNT-fenton	IWI	Temperature = 200 °C Pressure = 10 bar H_2/CO = 2/1 G H S V = 1066 h-1	Fixed bed	186.9	0.65	--	4.5	XCO = 68% FTS rate = 0.26 $g_{HC}\ g^{-1}h^{-1}$ C_5^+ = 62.9% C_2-C_4 = 21.6% CH_4 = 12.5%	[94]
15	Fe/CNT	IWI	Temperature = 270 °C Pressure = 20 bar H_2/CO = 1 G H S V = 4500 mL/g h	Fixed bed stainless steel	196	0.53	11.0	--	XCO = 32% C_5^+ = 73.0% C_2-C_4 = 11.8% C_{10}-C_{20} = 32.4% CH_4 = 15.2% CO_2 = 13.4% Hydrocarbon time yield = 0.102 α = 0.76	[38]
16	Fe/CNT-NaU	As above	As above	As above	200	0.39	7.5	--	XCO = 60% C_5^+ = 90.8% C_2-C_4 = 4.8% C_{10}- C_{20} = 52.0% CO_2 = 37.7% CH_4 = 4.4% α =0.89	[38]
17	Fe/CNT	Deposition precipitation	Temperature = 275 °C Pressure = 8 bar CO/H_2 = 1:2 G H S V = 2400 h-1	Fixed bed microreactor	123	0.28	--	5-11	XCO = 46.4% metal time yield = 35.8 C_5^+ = 57.4% C_1 = 29.1% C_2-C_4 = 13.5% CO_2 = 9.36% O/O+P = 0.023 α = 0.53	[95]
18	Fe-24 / NaCNT	As above	As above	As above	85	--	--	--	XCO = 71% metal time yield = 61.2 C_5^+ = 71.8% C1 = 6.0% C_2-C_4 = 21.6% CO_2 = 14.24% O/O+P = 0.78 α = 0.74	[95]
19	Fe-3Li/ CNT	As above	As above	As above	106	0.31	--	7-13	XCO = 62.2% metal time yield = 54.8 C_5^+=52.2% C1 = 30.2%, C_2-C_4 = 17.6% CO_2 = 10.31% O/O+P = N/A α = 0.52	[95]

Continuation Table

Entry	Catalyst	Preparation method	Conditions	Reactor	Surface area (m^2/g)	Ore volume (cm^3/g)	Ore size distribution (nm)	Particle size (nm)	Results	Ref.
20	Fe-3K/ CNT	As above	As above	As above	89	0.30	--	8-12	XCO = 38.4% metal time yield = 28.8% C_5^+ = 56.6% C_1 = 13.6% C_2-C_4 = 29.9% CO_2 = 8.52%, O/O+P = 0.39 α = 0.68	[95]
21	Fe/CNT-in	IWI	Temperature = 350 °C Pressure = 1 bar H_2/CO = 1:1 GHSV = 3.4 L/g.h TOS = 10 h	Fixed bed	192.9	0.52	--	4.9	XCO = 8.6% FTY activity = 1.5×10^{-5} mol g^{-1} s^{-1} C_5^+ = 16.0% C_2^o-C_4^o = 11.7% C_2^p-C_4^p = 40.4% CH_4 = 31.9% CO_2 = 29.2% P/O = 3.45	[33]
22	FeBi/ CNT-in	As above	As above	As above	183.3	0.52	--	5.1	XCO = 25.6% FTY activity = 4.7×10^{-5} mol g^{-1} s^{-1} C_5^+ = 4.6% C_2^o-C_4^o = 6.5% C_2^p-C_4^p = 62.4% CO_2 = 37.3% CH_4 = 27.0% P/O = 9.60	[33]
23	FePb/ CNT-in	As above	As above	As above	187.8	0.50	--	5.3	XCO = 35.9% FTY activity = 6.6×10^{-5} mol g^{-1} s^{-1} C_5^+ = 7.6% C_2^p-C_4^p = 58.9% C_2^o-C_4^o = 7.4% CH_4 = 26.1% CO_2 = 39.9% P/O = 7.96	[33]

--: Not found; IWI: Incipient wetness impregnation; CVD: Chemical vapour deposition; GHSV: Gas hourly space velocity; α: Alpha value; TOF: Turnover frequency; XCO: Carbon monoxide conversion

4. Iron Carbon-Supported catalysts modification in FTS

Carbon supports are known to be inert on their surfaces. Carbon supports have been used in FTS without any functionalization or promoters. Some researchers have seen low selectivities on inert carbon supports as compared with modified carbon supports[88,96]. For example, in **entry 6 Table 5**, Fe/CNT had lower selectivity towards C_5^+ of 59.0% as compared with **entry 7 Table 5**, Fe/CNT-Na where carbon nanotube support has been made chemically active with promoter sodium which showed a high selectivity of C_5^+ of 88.5%. To tune this property of inertness functionalization or promoters are used. These modifications make the surface of carbon supports to be chemically active[21]. For instance, nitrogen functional groups can act as nucleation sites for catalytic species which improves

stability and dispersion, and the promoters can alter the electronic properties of the supports[21,96].

Table 5. Iron supported catalysts, reaction conditions and modifications used on the catalysts and FTS performance

Catalyst	Reaction conditions	Modifications		Selectivity (%)		Ref.
		Functional group	Promoter	C_2-C_4	C_5^+	
Fe_5C_2@C/NPC	T = 340 °C P = 1.5 Mpa H_2/CO = 1 GHSV = 42 NL • g^{-1} • h^{-1}	N	-	-	33.5	[93]
Fe_3C@C	T = 320 °C P = 20 bar H_2/CO = 1 GHSV = 15000 $mlg^{-1}h^{-1}$	-	-	31.0	-	[89]
2K-Fe_3C@C	As above	-	K	41.9	-	[89]
Fe/rGO	T = 340 °C P = 20 bar H_2/CO = 1	-	-	31	0.3	[88]
FeK2/rGO	As above	-	K	68	6.7	[88]
Fe/CNTs	T = 270 °C P = 2 Mpa H_2/CO = 1 WHSV = 4500 h^{-1}	-	-	6.4	59.0	[98]
Fe/CNTs-Na	As above	-	Na	2.6	88.5	[98]
Fe@CNT	T = 370 °C P = 15 bar H_2/CO_2 = 3:1 8 Sccm	-	-	62.5	3.5	[99]
Fe@NCNT	As above	N	-	46.6	0.3	[99]
Na-Fe@NCNT	As above	N	Na	52.5	20.0	[99]
Fe/OCNT	T = 340 °C P = 25 bar H_2/CO = 1 GHSV = 50 $Lg^{-1}h^{-1}$	O	-	15.4		[20]
Fe/NCNT	As above	N	-	20.4		[20]
9Fe/CNF	T = 340 °C P = 20 bar H_2/CO = 1 GHSV = 54000 h^{-1}	-	Na & S	60	27	[76]
Fe/NCSver	T = 275 °C P = 8 bar	N	-	26.1	51.6	[100]
Fe-AC	T = 320 °C P = 2 Mpa H_2/CO = 1 GHSV = 3000 h^{-1}	-	-	16.0	37.4	[4]
Fe-10MnK-AC	As above	-	Mn & K	39.4	29.7	[4]
Fe-AC	T = 320 °C P = 2 Mpa H_2/CO = 0.97 GHSV = 15000 h^{-1}	-	-	31.2	16.5	[67]

Continuation Table

Catalyst	Reaction conditions	Modifications		Selectivity (%)		Ref.
		Functional group	Promoter	C_2-C_4	C_5^+	
FeN-AC	T = 320 °C P = 2 Mpa H_2/CO = 1 GHSV = 15000 h^{-1}	N	-	30.8	18.1	[67]
FeN-10MnKAC	T = 320 °C P = 2 Mpa H_2/CO = 0.46 GHSV = 15000 h^{-1}	N	Mn & K	44.7	23.9	[67]
15.7Fe-0.94K/AC (0Cu)	T = 280 °C P = 300 psig H_2/CO = 0.68 GHSV = 3 NLg^{-1}	-	K	34.9	56.5	[71]
15.7Fe-2Cu-0.94K/AC (2Cu)	T = 280 °C P = 300 psig H_2/CO = 0.67 GHSV = 3 NLg^{-1}	-	Cu & K	35.2	56.9	[71]
Fe/NMCs	T = 260 °C P = 1 Mpa H_2/CO = 1 W/F = 5 (g • h/mol)	N	-	-	67.0	[48]

Supports that have excellent properties are important for catalysis. The supports should have large surface area, good porosity. They should also have other structural properties such as the confinement effect in the case of CNTs, a high degree of graphitization as in the case of graphene, and moderate metal-support interaction. These properties are optimized for excellent performance of the catalysts in FTS. In addition to these carbon supports' structural properties, modifications with functional groups, promoters and heat treatments are used to further enhance iron carbon supported catalysts' performance in FTS[96,97]. The carbon supports can be functionalized with hetero atoms such as oxygen and nitrogen groups[67]. The addition of promoters such as alkali metals sodium and potassium, as well as other metals such as nickel, lanthanium and noble metals such as gold and platinum have been used to improve selectivity and activity in FTS[97]. Heat treatments have also been used to modify the properties of the iron based catalyst in FTS[41].

4.1 Functional Groups Effect in FTS

The effect of functional groups has been studied by several researchers in FTS[67,101]. Functional groups such as nitrogen and oxygen have been found to have an effect on the structure of carbon supports[67]. Functionalization with these groups increases the number of defects and nitrogen functional group can donate electrons (electron donor effect) on the carbon supports[38,67]. The defects act as nucleation sites in these supports, which helps in the anchoring of catalytic metals. The defects also help to improve the catalytic metals dispersion on the surface of the carbon support. This is excellent for catalysis as many of the active sites of the catalysts are exposed[68]. In some instances, the functionalized carbon supports tend to promote reduction at a lower temperature compared to pristine supports[68].

The functionalization effects of iron-based catalysts in FTS are summerized in **Table 5**. For instance, looking at **Table 5**, consider entries 8, 9 and 10, the catalysts Fe@CNT pristine, Fe@NCNT with functional group nitrogen, and catalyst Na-Fe@NCNT with nitrogen functional group as well as sodium promoters. The catalyst Fe@CNT had the largest C_2-C_4 selectivity of 62.5%, followed by the catalyst Na-Fe@NCNT with selectivity of 52.5% and lastly the catalyst Fe@NCNT with 46.6% selectivity. Considering the same products, the C_5^+ selectivity of the catalysts were: Na-Fe@NCNT with 20.0%; Fe@CNT with 3.5%; Fe@NCNT with 0.3%. The pristine catalyst performed well as regards C_2-C_4 selectivity because in some instances the functional groups bind strongly to the active sites of the catalysts, decreasing the number of sites for catalysis. The catalyst Na-Fe@NCNT performed best with respect to C_5^+. This may be because the introduction of sodium as a promoter may have interacted with the

support and the nitrogen functional group, which may in turn have reduced the interaction between nitrogen and the support. Nitrogen would then have minimal interaction with the iron catalytic metal, resulting in a many active sites being exposed for catalysis, compared to the catalyst Fe@NCNT.

Researchers should be careful when using functional groups as modification. The functional groups can bind strongly to the catalytic sites of the catalyst leaving only small numbers of active sites for catalysis[57]. This phenomenon is observed as indicated by lower selectivity and activity in FTS as revealed by **Table 5**.

4.2 Promoter Effect in FTS

Promoters such as alkali, alkaline and noble metals have been used by researchers in FTS[53,71,72]. Promoters like potassium can also increase the numbers of defects on the carbon supports[4,72]. In addition, the promoters also facilitate the formation of iron carbides during the preparation of the catalysts[4]. The promoters enrich the surface of the catalyst with electrons, which makes it hard for hydrogen to hydrogenate the unsaturated intermediates[66,89]. Promoters such as potassium supress the production of methane, methanol and the secondary hydrogenation of lower olefins[4]. In other studies promoters such as copper (2wt%) on the catalyst Fe-K/AC were found to enhance iron reduction[71]. By contrast a study performed by Xiong *et al*.[95] showed the opposite results when Na and K were used as promoters in the catalyst Fe/CNT. The addition of Na and K hindered the reducibility of the catalyst Fe/CNT by increasing the reduction temperature[95]. The promotion of the catalyst Fe-Cu-K/AC with Mo (6wt%) showed to have increased iron dispersion as well as decreasing iron carbide particle size[71,102]. The catalyst showed high stability in the reaction conditions and high activity. This was due to the addition of Mo, which prevented the agglomeration of iron carbide, and a larger number of active sites were then exposed in this catalyst.

The promoter effects in FTS are summerized in **Table 5. Entries 6 and 7 in Table 5** for catalysts Fe@/CNT-Na and Fe@/CNT were compared in terms of selectivity to C_5^+. The catalyst Fe@/CNT-Na had a C_5^+ selectivity of 88.5% compared to the Fe@/CNT catalyst with a selectivity of 59.0%. The catalyst Fe@/CNT-Na had excellent selectivity because of the sodium promoter, which provided an electron-rich surface on the prepared catalyst[53,89]. The sodium promoter also facilitated the formation of iron carbide, which is known to be the active phase in FTS[76].

The promoters are of excellent use in FTS, as they promote the formation of iron carbide, which is the main active phase for catalysis. On the other hand, large amounts of promoters can lead to an increase in the size of iron carbide particles and the blocking of the active sites resulting in lower selectivity and activity being observed[72].

4.3 Heat Treatment Effect in FTS

Functional groups and promoters as well as heat treatments improve catalyst properties. Heat treatment can improve functionalization on the catalyst[65]. Some researchers have found that upon heating polymeric mesoporous carbon containing iron at elevated temperatures, the carbides phase was formed (θ-Fe_3C, χ-Fe_5C_2)[65]. The carbides are an important active phase in FTS. The catalysts FeCP500, FeCP600 and FeCP700 were prepared at different calcination temperatures of 500 °C, 600 °C and 700 °C. The catalysts FeCP500, FeCP600 and FeCP700 had C_5-C_9 selectivity of 34.3%, 37.1% and 41.0%, respectively. The reaction conditions were a temperature of 270 °C and a pressure of 30 atmospheres[65]. Other researchers have performed pre-treatment of the catalyst Fe/GO-500 at 500 °C for 2 h[41]. Argon pre-treatment at 500 °C increased the surface area and defects and also weakened the Fe-GO metal-support interaction, which exposed more catalytically active sites[41]. The catalysts Fe/GO-300 and Fe/GO-500 had a C_5^+ selectivity of 22% and 37.7%, respectively. The catalyst Fe/GO-500 had high selectivity because of improved reduction, carburization and high stability in the reaction conditions[41].

5. Carbon Foam

Though carbon-based materials have been used in FTS, most researchers do not emphasize the importance of thermal and mechanical properties of these supports[93]. Hot spot formation has caused many researchers to introduce different strategies to solve this problem, such as the use of nitrogen in the syngas feed to reduce heat generated[103,104]. The problem accompanying the addition of nitrogen is that total pressure should be

increased appropriately. If not, there will be a loss of productivity. The commercial gasifiers produce syngas with very low numbers of inlets (< 1%), so it is unlikely this approach could be used in industrial reactors[103]. In addition, the recycling of the hydrocarbons produced has been used to remove excess heat[103,104]. Both strategies consume time and resources.

The CFs are carbonaceous materials that have three-dimensional reticular structures of various shapes and sizes. CFs have been under-utilized in applications, based on their unique and tunable properties, such as high mechanical strength and high thermal conductivity. The CFs are synthesized using blowing and carbonization, template carbonization, compression of exfoliated graphite, and the assembly of graphene nanosheets[105]. **Figure 7** depicts an example of carbon foam.

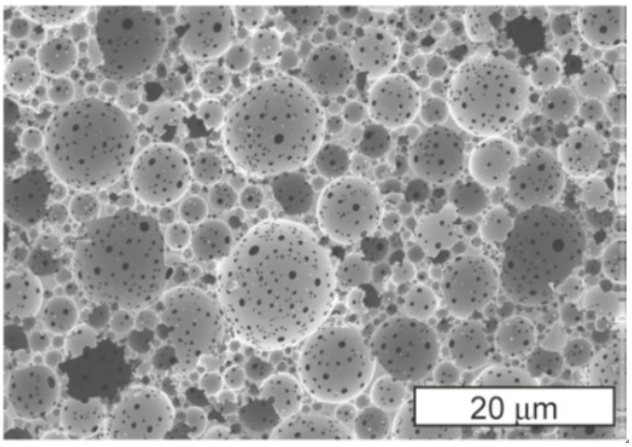

Figure 7. SEM image of carbon foam[106]

The CFs have good structural properties such as thermal conductivity and mechanical strength, high surface area and porosity as indicated in **Table 6**. The thermal and mechanical properties of carbon foams are strongly dependent on the raw material used during synthesis. CFs can be prepared from various carbon sources, which can affect mechanical and thermal conductivity differently. That being said, it has a wide range of thermal conductivity and mechanical strengths[107,108].

Table 6. Structural properties of carbon foams from different authors.

BET (m^2/g)	V_{total} (cm^3/g)	D (nm)	Thermal conductivity W/(m·K)	Electrical conductivity (S/cm)	Mechanical strength (KPa)	Young modulus (MPa)	Porosity (%)	Ref.
1158	0.598	2.1	—	—	—	—	—	[109]
—	—	—	—	700	700	72.93	70	[110]
—	—	—	50-150	—	—	—	—	[111]

The CFs properties are easily tunable during synthesis by adjusting parameters like temperature, pressure and release time. The thermal conductivity and mechanical strength are greatly improved by carbonization and graphitization of CFs at a high temperature. Carbonization is performed at temperatures of 1000 °C, while graphitization is carried out at a temperature of 2000 oC to 2800 °C. These three parameters affect the porosity, the thermal and electrical conductivity, as well as the mechanical strength of CFs. Most importantly, it is simple and cheap to prepare CFs compared to other nanostructured carbon materials that are even higher in cost than conventional oxides supports[15]. **Table 6** shows some properties of carbon foams, derived from different studies.

Carbon foam applications include use in batteries, sensors, supercapacitors, oxygen reduction, microwave absorption and water treatment[111]. This material has displayed excellent results in applications where it has been used for excess heat removal because of its high thermal and electrical conductivity and high mechanical strength[111].

6. Conclusions and Future Perspectives

The structural properties of carbon supports have been linked to their function in FTS. The carbon supports exhibit weak metal-support interaction. The large percentages of promoters lead to strong metal-support interaction. The CNTs and OMCs have a confining ability, while CSs act as nanoreactors that protect catalytic metals from being easily deactivated. The studies reviewed show that the iron-based catalysts inside the CNTs are more stable, compared to catalysts on the outside of the tube. The confined catalysts can be used for longer periods on stream and are recyclable, which is vital for chemical industries in terms of environmental pollution. The defects on graphene act as nucleation sites that facilitate anchoring and maximum dispersion of the iron nanoparticles. The catalysts properties are highly interrelated for good activity and selectivity in FTS. Particle size effect is crucial in FTS but there are still controversies in studies hence more studies are still needed to bring clarification into this important issue. It is very important that iron oxides are reduced into iron carbides. These carbides studies have shown that are important as are most active phase in iron catalysts which are linked to excellent activity and selectivity in FTS.

The carbon support modifications lead to improved FTS performance. The functional groups act as the anchoring sites and increase the defects on the carbon support, which is important for metal dispersion. The well-dispersed catalysts have a high selectivity and activity, as active sites are exposed for catalysis. On the other hand, the promoters make the surface of the catalyst electron-rich, which makes it difficult for hydrogen to hydrogenate the unsaturated intermediates. The promoters facilitate the formation of iron carbide, the active phase in FTS. Heat treatment improves the properties of the catalyst, which enhances selectivity and activity in FTS.

Large percentages of functional groups in the catalysts bind strongly to the active phase, which leads to lower selectivity and activity, as well as catalyst deactivation. The large percentage of promoters increases the size of the active phase and blocks the active sites of the catalyst. This results in poor performance in FTS because of the growth in particle size and carbon deposition. Researchers should thoroughly study the relationship between functional groups and promoters as shown by **Table 5 entries 8-10**.

This review shows that high thermal conductivity and mechanical strength are crucial in reactions performed at a high temperature. Supports with high thermal conductivity absorb the excess heat generated during the reaction, which improves the catalyst stability. High mechanical strength is important in harsh reaction conditions as it prevents decomposition of the support, which leads to catalyst deactivation. Researchers pay little attention to the thermal conductivity and mechanical strength of carbon supports. The confinement effect still poses a great challenge as to how to deposit iron nanoparticles inside the CNTs and OMCs' channels.

Researchers should explore the unique properties of carbon foam. The high thermal conductivity and mechanical strength of carbon foams have been clearly demonstrated in other fields such as in supercapacitors. In general, carbon foams have been used in heat management.

Acknowledgments

The authors are grateful to the University of South Africa (UNISA) and National Research Foundation (NRF 132152 and 137947) for the financial support provided to support this research work.

Conflict of Interest

The authors declare that they have no known competing financial interests or personal relationships that could influence the work reported in this paper.

References

[1] Davari M, Karimi S, Tavasoli A, *et al*. Enhancement of activity, selectivity and stability of CNTs-supported cobalt catalyst in Fischer-Tropsch via CNTs functionalization. *Applied Catalysis A: General*, 2014;485:133-142. https://doi.org/10.1016/j.apcata.2014.07.023

[2] Cheng K, Ordomsky VV, Virginie M, *et al*. Support effects in high temperature Fischer-Tropsch synthesis on iron catalysts. *Applied Catalysis A: General*, 2014;488:66-77. https://doi.org/10.1016/j.apcata.2014.09.033

[3] Aluha J, Boahene P, Dalai A, *et al*. Synthesis and

characterization of Co/C and Fe/C nanocatalysts for Fischer-Tropsch synthesis: a comparative study using a fixed-bed reactor. *Industrial & Engineering Chemistry Research*, 2015;54(43):10661-10674. https://doi.org/10.1021/acs.iecr.5b03003

[4] Tian Z, Wang C, Si Z, *et al*. Fischer-Tropsch synthesis to light olefins over iron-based catalysts supported on KMnO4 modified activated carbon by a facile method. *Applied Catalysis A: General*, 2017;541:50-59. https://doi.org/10.1016/j.apcata.2017.05.001

[5] Qin C, Hou B, Wang J, *et al*. Stabilizing optimal crystalline facet of cobalt catalysts for Fischer-Tropsch synthesis. *ACS Applied Materials & interfaces*, 2019;11(37):33886-33893. https://doi.org/10.1021/acsami.9b10174

[6] Bengoa JF, Alvarez AM, Cagnoli MV, *et al*. Influence of intermediate iron reduced species in Fischer-Tropsch synthesis using Fe/C catalysts. *Applied Catalysis A: General*, 2007;325(1):68-75. https://doi.org/10.1016/j.apcata.2007.03.012

[7] Chernyak SA, Suslova EV, Ivanov AS, *et al*. Co catalysts supported on oxidized CNTs: evolution of structure during preparation, reduction and catalytic test in Fischer-Tropsch synthesis. *Applied Catalysis A: General*, 2016;523:221-229. https://doi.org/10.1016/j.apcata.2016.06.012

[8] Maillard F, Simonov PA and Savinova ER. Carbon materials as supports for fuel cell electrocatalysts. Carbon Materials for Catalysis; 2009. p. 429-480.

[9] Chen Y, Wei J, Duyar MS, *et al*. Carbon-based catalysts for Fischer-Tropsch synthesis. *Chemical Society Reviews*, 2021;50(4):2337-2366. https://doi.org/10.1039/d0cs00905a

[10] Li M and Mu B. Effect of different dimensional carbon materials on the properties and application of phase change materials: a review. *Applied Energy*, 2019;242:695-715. https://doi.org/10.1016/j.apenergy.2019.03.085

[11] Coville NJ, Mhlanga SD, Nxumalo EN, *et al*. A review of shaped carbon nanomaterials. *South African Journal of Science*, 2011;107(3):1-15. https://doi.org/10.4102/sajs.v107i3/4.418

[12] Diehl F and Khodakov AY. Promotion of cobalt Fischer-Tropsch catalysts with noble metals: a review. *Oil & Gas Science and Technology-Revue de l'IFP*, 2009;64(1):11-24. https://doi.org/10.2516/ogst:2008040

[13] Wu B, Kuang Y, Zhang X, *et al*. Noble metal nanoparticles/carbon nanotubes nanohybrids: synthesis and applications. *Nano Today*, 2011;6(1):75-90. https://doi.org/10.1016/j.nantod.2010.12.008

[14] Fu T and Li Z. Review of recent development in Co-based catalysts supported on carbon materials for Fischer-Tropsch synthesis. *Chemical Engineering Science,* 2015;135:3-20. https://doi.org/10.1016/j.ces.2015.03.007

[15] Valero-Romero MJ, Rodríguez-Cano MÁ, Palomo J, *et al*. Carbon-based materials as catalyst supports for Fischer-Tropsch synthesis: a review. *Frontiers in Materials*, 2021;7:617432. https://doi.org/10.3389/fmats.2020.617432

[16] Kennedy Oubagaranadin JU and Murthy ZVP. Activated carbon classifications, properties and applications. In: Cacioppo LM (editor). Chemistry research summaries. New York: Nova; 2012. pp. 93-94.

[17] Auer E, Freund A, Pietsch J, *et al*. Carbons as supports for industrial precious metal catalysts. *Applied Catalysis A: General*, 1998;173(2):259-271. https://doi.org/10.1016/S0926-860X(98)00184-7

[18] Liu M, Zhang R and Chen W. Graphene-supported nanoelectrocatalysts for fuel cells: synthesis, properties, and applications. *Chemical Reviews*, 2014;114(10):5117-5160. https://doi.org/10.1021/cr400523y

[19] Menard D, Py X and Mazet N. Activated carbon monolith of high thermal conductivity for adsorption processes improvement: Part A: Adsorption step. *Chemical Engineering and Processing: Process Intensification*, 2005;44(9):1029-1038. https://doi.org/10.1016/j.cep.2005.02.002

[20] Chew LM, Xia W, Düdder H, *et al*. On the role of the stability of functional groups in multi-walled carbon nanotubes applied as support in iron-based high-temperature Fischer-Tropsch synthesis. *Catalysis Today*, 2016;270:85-92. https://doi.org/10.1016/j.cattod.2015.09.023

[21] Lama SMG, Weber JL, Heil T, *et al*. Tandem promotion of iron catalysts by sodium-sulfur and nitrogen-doped carbon layers on carbon

nanotube supports for the Fischer-Tropsch to olefins synthesis. *Applied Catalysis A: General*, 2018;568:213-220. https://doi.org/10.1016/j.apcata.2018.09.016

[22] Balandin AA, Ghosh S, Bao W, *et al*. Superior thermal conductivity of single-layer graphene. *Nano Letters*, 2008;8(3):902-907. https://doi.org/10.1021/nl0731872

[23] Singh SK, Singh MK, Kulkarni PP, *et al*. Amine-modified graphene: thrombo-protective safer alternative to graphene oxide for biomedical applications. *ACS Nano*, 2012;6(3):2731-2740. https://doi.org/10.1021/nn300172t

[24] Serp P and Philippot K. Nanomaterials in Catalysis. 1st ed. New York: Wiley; 2012. p. 1-54.

[25] Anwer MAS and Naguib HE. Study on the morphological, dynamic mechanical and thermal properties of PLA carbon nanofibre composites. *Composites Part B: Engineering*, 2016;91:631-639. https://doi.org/10.1016/j.compositesb.2016.01.039

[26] Yuan G, Li X, Dong Z, *et al.* Pitch-based ribbon-shaped carbon-fiber-reinforced one-dimensional carbon/carbon composites with ultrahigh thermal conductivity. *Carbon*, 2014;68:413-425. https://doi.org/10.1016/j.carbon.2013.11.018

[27] Xiong H, Jewell LL and Coville NJ. Shaped carbons as supports for the catalytic conversion of syngas to clean fuels. *ACS Catalysis*, 2015;5(4):2640-2658. https://doi.org/10.1021/acscatal.5b00090

[28] Wang LW, Tamainot-Telto Z, Thorpe R, et al. Study of thermal conductivity, permeability, and adsorption performance of consolidated composite activated carbon adsorbent for refrigeration. *Renewable Energy*, 2011;36(8):2062-2066. https://doi.org/10.1016/j.renene.2011.01.005

[29] Sun Z, Sun B, Qiao M, *et al*. A general chelate-assisted co-assembly to metallic nanoparticles-incorporated ordered mesoporous carbon catalysts for Fischer-Tropsch synthesis. *Journal of the American Chemical Society*, 2012;134(42):17653-17660. https://doi.org/10.1021/ja306913x

[30] Cruz MGA, Bastos-Neto M, Oliveira AC, *et al*. On the structural, textural and morphological features of Fe-based catalysts supported on polystyrene mesoporous carbon for Fischer-Tropsch synthesis. *Applied Catalysis A: General*, 2015;495:72-83. https://doi.org/10.1016/j.apcata.2015.02.009

[31] Kim KK, Reina A, Shi Y, *et al*. Enhancing the conductivity of transparent graphene films via doping. *Nanotechnology*, 2010;21(28):285205. https://doi.org/10.1088/0957-4484/21/28/285205

[32] Menon M, Andriotis AN and Froudakis GE. Curvature dependence of the metal catalyst atom interaction with carbon nanotubes walls. *Chemical Physics Letters*, 2000;320(5-6):425-434. https://doi.org/10.1016/S0009-2614(00)00224-4

[33] Gu B, He S, Peron DV, *et al*. Synergy of nanoconfinement and promotion in the design of efficient supported iron catalysts for direct olefin synthesis from syngas. *Journal of Catalysis*, 2019;376:1-16. https://doi.org/10.1016/j.jcat.2019.06.035

[34] Chen W, Fan Z, Pan X, *et al*. Effect of confinement in carbon nanotubes on the activity of Fischer-Tropsch iron catalyst. J*ournal of the American Chemical Society*, 2008;130(29):9414-9419. https://doi.org/10.1021/ja8008192

[35] Bahome MC, Jewell LL, Hildebrandt D, *et al*. Fischer-Tropsch synthesis over iron catalysts supported on carbon nanotubes. *Applied Catalysis A: General*, 2005;287(1):60-67. https://doi.org/10.1016/j.apcata.2005.03.029

[36] Chen Q, Liu G, Ding S, *et al*. Design of ultra-active iron-based Fischer-Tropsch synthesis catalysts over spherical mesoporous carbon with developed porosity. *Chemical Engineering Journal*, 2018;334:714-724. https://doi.org/10.1016/j.cej.2017.10.093

[37] Casavola M, Hermannsdörfer J, de Jonge N, *et al*. Fabrication of Fischer-Tropsch catalysts by deposition of iron nanocrystals on carbon nanotubes. *Advanced Functional Materials*, 2015;25(33):5309-5319. https://doi.org/10.1002/adfm.201501882

[38] Liu R, Liu R, Ma X, *et al*. Efficient diesel production over the iron-based Fischer-Tropsch catalyst supported on CNTs treated by urea/NaOH. *Fuel*, 2018;211:827-836. https://doi.org/10.1016/j.fuel.2017.09.114

[39] Karimi S, Tavasoli A, Mortazavi Y, *et al*. Cobalt supported on Graphene-a promising novel Fischer-

Tropsch synthesis catalyst. *Applied Catalysis A: General*, 2015;499:188-196. https://doi.org/10.1016/j.apcata.2015.04.024

[40] Dlamini MW, Kumi DO, Phaahlamohlaka TN, *et al*. Carbon spheres prepared by hydrothermal synthesis-a support for bimetallic iron cobalt Fischer-Tropsch catalysts. *ChemCatChem*, 2015;7(18):3000-3011. https://doi.org/10.1002/cctc.201500334

[41] Wei Y, Zhang C, Liu X, *et al*. Enhanced Fischer-Tropsch performances of graphene oxide-supported iron catalysts via argon pretreatment. *Catalysis Science & Technology*, 2018;8(4):1113-1125. https://doi.org/10.1039/c7cy02449e

[42] Yang Y, Jia L, Meng Y, *et al*. Fischer-Tropsch synthesis over ordered mesoporous carbon supported cobalt catalysts: the role of amount of carbon precursor in catalytic performance. *Catalysis Letters*, 2012;142(2):195-204. https://doi.org/10.1007/s10562-011-0747-3

[43] Zaman M, Khodadi A and Mortazavi Y. Fischer-Tropsch synthesis over cobalt dispersed on carbon nanotubes-based supports and activated carbon. *Fuel Processing Technology*, 2009;90(10):1214-1219. https://doi.org/10.1016/j.fuproc.2009.05.026

[44] Deshmukh AA, Mhlanga SD and Coville NJ. Carbon spheres. *Materials Science and Engineering: R: Reports*, 2010;70(1-2):1-28. https://doi.org/10.1016/j.mser.2010.06.017

[45] Cheng Q, Zhao N, Lyu S, *et al*. Tuning interaction between cobalt catalysts and nitrogen dopants in carbon nanospheres to promote Fischer-Tropsch synthesis. *Applied Catalysis B: Environmental*, 2019;248:73-83. https://doi.org/10.1016/j.apcatb.2019.02.024

[46] Reina A, Jia X, Ho J, *et al*. Large area, few-layer graphene films on arbitrary substrates by chemical vapor deposition. *Nano Letters*, 2009;9(1):30-35. https://doi.org/10.1021/nl801827v

[47] Lee HK, Lee JH, Seo JH, *et al*. Extremely productive iron-carbide nanoparticles on graphene flakes for CO hydrogenation reactions under harsh conditions. *Journal of Catalysis*, 2019;378:289-297. https://doi.org/10.1016/j.jcat.2019.09.004

[48] Liu G, Chen Q, Oyunkhand E, *et al*. Nitrogen-rich mesoporous carbon supported iron catalyst with superior activity for Fischer-Tropsch synthesis. *Carbon*, 2018;130:304-314. https://doi.org/10.1016/j.carbon.2018.01.015

[49] Ghogia AC, Nzihou A, Serp P, *et al*. Cobalt catalysts on carbon-based materials for Fischer-Tropsch synthesis: a review. *Applied Catalysis A: General*, 2021;609:117906. https://doi.org/10.1016/j.apcata.2020.117906

[50] de Smit E and Weckhuysen BM. The renaissance of iron-based Fischer-Tropsch synthesis: on the multifaceted catalyst deactivation behaviour. *Chemical Society Reviews*, 2008;37(12):2758-2781. https://doi.org/10.1039/b805427d

[51] Pendyala VRR, Graham UM, Jacobs G, *et al*. Fischer-Tropsch synthesis: deactivation as a function of potassium promoter loading for precipitated iron catalyst. *Catalysis Letters*, 2014;144(10):1704-1716. https://doi.org/10.1007/s10562-014-1336-z

[52] Paalanen PP and Weckhuysen BM. Carbon pathways, sodium-sulphur promotion and identification of iron carbides in iron-based Fischer-Tropsch synthesis. *ChemCatChem*, 2020;12(17):4202-4223. https://doi.org/10.1002/cctc.202000535

[53] Asami K, Komiyama K, Yoshida K, *et al*. Synthesis of lower olefins from synthesis gas over active carbon-supported iron catalyst. *Catalysis Today*, 2018;303:117-122. https://doi.org/10.1016/j.cattod.2017.09.010

[54] Torres Galvis HM, Bitter JH, Davidian T, *et al*. Iron particle size effects for direct production of lower olefins from synthesis gas. *Journal of the American Chemical Society*, 2012;134(39):16207-16215. https://doi.org/10.1021/ja304958u

[55] Joo SH, Jun S and Ryoo R. Synthesis of ordered mesoporous carbon molecular sieves CMK-1. *Microporous and Mesoporous Materials*, 2001;44:153-158. https://doi.org/10.1016/S1387-1811(01)00179-2

[56] Cheng Y, Tian J, Lin J, *et al*. Potassium-promoted magnesium ferrite on 3D porous graphene as highly efficient catalyst for CO hydrogenation to lower

olefins. *Journal of Catalysis*, 2019;374:24-35. https://doi.org/10.1016/j.jcat.2019.04.024

[57] Xiong H, Motchelaho MA, Moyo M, *et al*. Fischer-Tropsch synthesis: iron-based catalysts supported on nitrogen-doped carbon nanotubes synthesized by post-doping. *Applied Catalysis A: General*, 2014;482:377-386. https://doi.org/10.1016/j.apcata.2014.06.019

[58] Abbaslou RMM, Tavassoli A, Soltan J, *et al*. Iron catalysts supported on carbon nanotubes for Fischer-Tropsch synthesis: effect of catalytic site position. *Applied Catalysis A: General*, 2009;367(1-2):47-52. https://doi.org/10.1016/j.apcata.2009.07.025

[59] Díaz JA, Akhavan H, Romero A, *et al*. Cobalt and iron supported on carbon nanofibers as catalysts for Fischer-Tropsch synthesis. *Fuel Processing Technology*, 2014;128:417-424. https://doi.org/10.1016/j.fuproc.2014.08.005

[60] van Steen E and Prinsloo FF. Comparison of preparation methods for carbon nanotubes supported iron Fischer-Tropsch catalysts. *Catalysis Today*, 2002;71(3-4):327-334. https://doi.org/10.1016/S0920-5861(01)00459-X

[61] Truong-Huu T, Chizari K, Janowska I, *et al*. Few-layer graphene supporting palladium nanoparticles with a fully accessible effective surface for liquid-phase hydrogenation reaction. *Catalysis Today*, 2012;189(1):77-82. https://doi.org/10.1016/j.cattod.2012.04.005

[62] Wang ZL and Kang ZC. Graphitic structure and surface chemical activity of nanosize carbon spheres. *Carbon*, 1997;35(3):419-426. https://doi.org/10.1016/S0008-6223(97)89613-3

[63] Paquin F, Rivnay J, Salleo A, *et al*. Multi-phase semicrystalline microstructures drive exciton dissociation in neat plastic semiconductors. arXiv preprint arXiv:1310.8002, 2013. https://doi.org/10.48550/arXiv.1310.8002

[64] Yang Y, Jia L, Hou B, *et al*. The oxidizing pretreatment-mediated autoreduction behaviour of cobalt nanoparticles supported on ordered mesoporous carbon for Fischer-Tropsch synthesis. *Catalysis Science & Technology*, 2014;4(3):717-728. https://doi.org/10.1039/c3cy00729d

[65] Cruz MGA, Fernandes FAN, Oliveira AC, *et al*. Effect of the calcination temperatures of the Fe-based catalysts supported on polystyrene mesoporous carbon for FTS Synthesis. *Catalysis Today*, 2017;282:174-184. https://doi.org/10.1016/j.cattod.2016.07.023

[66] Kangvansura P, Chew LM, Saengsui W, *et al*. Product distribution of CO_2 hydrogenation by K-and Mn-promoted Fe catalysts supported on N-functionalized carbon nanotubes. *Catalysis Today*, 2016;275:59-65. https://doi.org/10.1016/j.cattod.2016.02.045

[67] Tian Z, Wang C, Si Z, *et al*. Enhancement of light olefins selectivity over N-doped Fischer-Tropsch synthesis catalyst supported on activated carbon pretreated with $KMnO_4$. *Catalysts*, 2019;9(6):505. https://doi.org/10.3390/catal9060505

[68] Li Z, Liu R, Xu Y, *et al*. Enhanced Fischer-Tropsch synthesis performance of iron-based catalysts supported on nitric acid treated N-doped CNTs. *Applied Surface Science*, 2015;347:643-650. https://doi.org/10.1016/j.apsusc.2015.04.169

[69] Abrokwah RY, Rahman MM, Deshmane VG, *et al*. Effect of titania support on Fischer-Tropsch synthesis using cobalt, iron, and ruthenium catalysts in silicon-microchannel microreactor. *Molecular Catalysis*, 2019;478:110566. https://doi.org/10.1016/j.mcat.2019.110566

[70] Numpilai T, Cheng CK, Limtrakul J, *et al*. Recent advances in light olefins production from catalytic hydrogenation of carbon dioxide. *Process Safety and Environmental Protection*, 2021;151:401-427. https://doi.org/10.1016/j.psep.2021.05.025

[71] Ma W, Kugler EL and Dadyburjor DB. Promotional effect of copper on activity and selectivity to hydrocarbons and oxygenates for Fischer-Tropsch synthesis over potassium-promoted iron catalysts supported on activated carbon. *Energy & Fuels*, 2011;25(5):1931-1938. https://doi.org/10.1021/ef101720c

[72] Oschatz M, Krans N, Xie J, *et al*. Systematic variation of the sodium/sulfur promoter content on carbon-supported iron catalysts for the Fischer-Tropsch to olefins reaction. *Journal of Energy Chemistry*, 2016;25(6):985-993. https://doi.org/10.1016/j.jechem.2016.10.011

[73] Ni Z, Qin H, Kang S, *et al*. Effect of graphitic carbon modification on the catalytic performance of Fe@SiO_2-GC catalysts for forming lower olefins via Fischer-Tropsch synthesis. *Journal of Colloid and Interface Science*, 2018;516:16-22. https://doi.org/10.1016/j.jcis.2018.01.017

[74] Wei Y, Luo D, Zhang C, *et al*. Precursor controlled synthesis of graphene oxide supported iron catalysts for Fischer-Tropsch synthesis. *Catalysis Science & Technology*, 2018;8(11):2883-2893. https://doi.org/10.1039/c8cy00617b

[75] Xiong H, Moyo M, Motchelaho MAM, *et al*. Fischer-Tropsch synthesis over model iron catalysts supported on carbon spheres: the effect of iron precursor, support pretreatment, catalyst preparation method and promoters. *Applied Catalysis A: General*, 2010;388(1-2):168-178. https://doi.org/10.1016/j.apcata.2010.08.039

[76] Xie J, Torres Galvis HM, Koeken ACJ, *et al*. Size and promoter effects on stability of carbon-nanofiber-supported iron-based Fischer-Tropsch catalysts. *ACS Catalysis*, 2016;6(6):4017-4024. https://doi.org/10.1021/acscatal.6b00321

[77] Bezemer GL, Bitter JH, Kuipers HPCE, *et al*. Cobalt particle size effects in the Fischer-Tropsch reaction studied with carbon nanofiber supported catalysts. *Journal of the American Chemical Society*, 2006;128(12):3956-3964. https://doi.org/10.1021/ja058282w

[78] Pendyala VRR, Jacobs G, Graham UM, *et al*. Fischer-Tropsch synthesis: influence of acid treatment and preparation method on carbon nanotube supported ruthenium catalysts. *Industrial & Engineering Chemistry Research*, 2017;56(22):6408-6418. https://doi.org/10.1021/acs.iecr.7b00341

[79] Teng X, Huang S, Wang J, *et al*. Fabrication of Fe_2C embedded in hollow carbon spheres: a high-performance and stable catalyst for Fischer-Tropsch synthesis. *ChemCatChem*, 2018;10(17):3883-3891. https://doi.org/10.1002/cctc.201800488

[80] Yang Z, Guo S, Pan X, *et al*. FeN nanoparticles confined in carbon nanotubes for CO hydrogenation. *Energy & Environmental Science*, 2011;4(11):4500-4503. https://doi.org/10.1039/c1ee01428e

[81] Kango S, Kalia S, Celli A, *et al*. Surface modification of inorganic nanoparticles for development of organic-inorganic nanocomposites-A review. *Progress in Polymer Science*, 2013;38(8):1232-1261. https://doi.org/10.1016/j.progpolymsci.2013.02.003

[82] Oschatz M, van Deelen TW, Weber JL, *et al*. Effects of calcination and activation conditions on ordered mesoporous carbon supported iron catalysts for production of lower olefins from synthesis gas. *Catalysis Science & Technology*, 2016;6(24): 8464-8473. https://doi.org/10.1039/c6cy01251e

[83] Oschatz M, Hofmann JP, van Deelen TW, *et al*. Effects of the functionalization of the ordered mesoporous carbon support surface on iron catalysts for the Fischer-Tropsch synthesis of lower olefins. *ChemCatChem*, 2017;9(4):620-628. https://doi.org/10.1002/cctc.201601228

[84] Mousavi S, Zamaniyan A, Irani M, *et al*. Generalized kinetic model for iron and cobalt based Fischer-Tropsch synthesis catalysts: review and model evaluation. *Applied Catalysis A: General*, 2015;506:57-66. https://doi.org/10.1016/j.apcata.2015.08.020

[85] Oschatz M, Lamme WS, Xie J, *et al*. Ordered mesoporous materials as supports for stable iron catalysts in the Fischer-Tropsch synthesis of lower olefins. *ChemCatChem*, 2016;8(17):2846-2852. https://doi.org/10.1002/cctc.201600492

[86] Eslava JL, Iglesias-Juez A, Fernández-García M, *et al*. Effect of different promoter precursors in a model Ru-Cs/graphite system on the catalytic selectivity for Fischer-Tropsch reaction. *Applied Surface Science*, 2018;447:307-314. https://doi.org/10.1016/j.apsusc.2018.03.207

[87] Terrones M, Botello-Méndez AR, Campos-Delgado J, *et al*. Graphene and graphite nanoribbons: morphology, properties, synthesis, defects and applications. *Nano Today*, 2010;5(4):351-372. https://doi.org/10.1016/j.nantod.2010.06.010

[88] Cheng Y, Lin J, Xu K, *et al*. Fischer-Tropsch synthesis to lower olefins over potassium-promoted reduced graphene oxide supported iron catalysts. *ACS Catalysis*, 2016;6(1):389-399. https://doi.org/10.1021/acscatal.5b02024

[89] Tian Z, Wang C, Yue J, *et al*. Effect of a potassium

promoter on the Fischer-Tropsch synthesis of light olefins over iron carbide catalysts encapsulated in graphene-like carbon. *Catalysis Science & Technology*, 2019;9(11):2728-2741. https://doi.org/10.1039/c9cy00403c

[90] Moussa SO, Panchakarla LS, Ho MQ, et al. Graphene-supported, iron-based nanoparticles for catalytic production of liquid hydrocarbons from synthesis gas: the role of the graphene support in comparison with carbon nanotubes. ACS Catalysis, 2014;4(2):535-545. https://doi.org/10.1021/cs4010198

[91] Marsh H and Reinoso FR. Activated carbon. 1st ed. Elsevier; 2006. p. 1-536.

[92] Chernavskii PA, Kazantsev RV, Pankina GV, *et al*. Carbon-silica composite as an effective support for iron Fischer-Tropsch synthesis catalysts. *Energy Technology*, 2019;7(4):1800961. https://doi.org/10.1002/ente.201800961

[93] Lee JH, Lee HK, Chun DH, *et al*. Phase-controlled synthesis of thermally stable nitrogen-doped carbon supported iron catalysts for highly efficient Fischer-Tropsch synthesis. *Nano Research*, 2019;12(10):2568-2575. https://doi.org/10.1007/s12274-019-2487-4

[94] Almkhelfe H, Li X, Thapa P, *et al*. Carbon nanotube-supported catalysts prepared by a modified photo-Fenton process for Fischer-Tropsch synthesis. *Journal of Catalysis*, 2018;361:278-289. https://doi.org/10.1016/j.jcat.2018.02.009

[95] Xiong H, Motchelaho MA, Moyo M, *et al*. Effect of Group I alkali metal promoters on Fe/CNT catalysts in Fischer-Tropsch synthesis. *Fuel*, 2015;150:687-696. https://doi.org/10.1016/j.fuel.2015.02.099

[96] Roe DP, Xu R and Roberts CB. Influence of a carbon nanotube support and supercritical fluid reaction medium on Fe-catalyzed Fischer-Tropsch synthesis. *Applied Catalysis A: General*, 2017;543:141-149. https://doi.org/10.1016/j.apcata.2017.06.020

[97] Wang T, Ding Y, Lü Y, *et al*. Influence of lanthanum on the performance of Zr-Co/activated carbon catalysts in Fischer-Tropsch synthesis. *Journal of Natural Gas Chemistry*, 2008;17(2):153-158. https://doi.org/10.1016/S1003-9953(08)60043-2

[98] Liu R, Xu Y, Li Z, *et al*. A facile and efficient modification of CNTs for improved Fischer-Tropsch performance on iron catalyst: alkali modification. *ChemCatChem*, 2016;8(8):1454-1458. https://doi.org/10.1002/cctc.201501219

[99] Williamson DL, Herdes C, Torrente-Murciano L, *et al*. N-Doped Fe@ CNT for combined RWGS/FT CO_2 hydrogenation. *ACS Sustainable Chemistry & Engineering*, 2019;7(7):7395-7402. https://doi.org/10.1021/acssuschemeng.9b00672

[100] Xiong H, Moyo M, Motchelaho MA, *et al*. Fischer-Tropsch synthesis: iron catalysts supported on N-doped carbon spheres prepared by chemical vapor deposition and hydrothermal approaches. *Journal of Catalysis*, 2014;311:80-87. https://doi.org/10.1016/j.jcat.2013.11.007

[101] Sun J, Guo L, Ma Q, *et al*. Functionalized natural carbon-supported nanoparticles as excellent catalysts for hydrocarbon production. *Chemistry-An Asian Journal*, 2017;12(3):366-371. https://doi.org/10.1002/asia.201601546

[102] Aluha J and Abatzoglou N. Promotional effect of Mo and Ni in plasma-synthesized Co-Fe/C bimetallic nano-catalysts for Fischer-Tropsch synthesis. *Journal of Industrial and Engineering Chemistry*, 2017;50:199-212. https://doi.org/10.1016/j.jiec.2017.02.018

[103] Todic B, Mandic M, Nikacevic N, *et al*. Effects of process and design parameters on heat management in fixed bed Fischer-Tropsch synthesis reactor. *Korean Journal of Chemical Engineering*, 2018;35(4):875-889. https://doi.org/10.1007/s11814-017-0335-3

[104] Sie ST and Krishna R. Fundamentals and selection of advanced Fischer-Tropsch reactors. *Applied Catalysis A: General*, 1999;186(1-2):55-70. https://doi.org/10.1016/S0926-860X(99)00164-7

[105] Tjandra R, Liu W, Lim L, *et al*. Melamine based, n-doped carbon/reduced graphene oxide composite foam for Li-ion hybrid supercapacitors. *Carbon*, 2018;129:152-158. https://doi.org/10.1016/j.carbon.2017.12.021

[106] Gross AF and Nowak AP. Hierarchical carbon foams with independently tunable mesopore and macropore size distributions. *Langmuir*,

2010;26(13):11378-11383. https://doi.org/10.1021/la1007846

[107] Liu H, Li T, Huang T, *et al*. Effect of multi-walled carbon nanotube additive on the microstructure and properties of pitch-derived carbon foams. *Journal of Materials Science*, 2015;50(23):7583-7590. https://doi.org/10.1007/s10853-015-9314-4

[108] Zhang S, Liu M, Gan L, *et al*. Synthesis of carbon foams with a high compressive strength from arylacetylene. *New Carbon Materials*, 2010;25(1):9-14. https://doi.org/10.1016/S1872-5805(09)60012-3

[109] Guo D, Ding B, Hu X, *et al*. Synthesis of boron and nitrogen codoped porous carbon foam for high performance supercapacitors. *ACS Sustainable Chemistry & Engineering*, 2018;6(9):11441-11449. https://doi.org/10.1021/acssuschemeng.8b01435

[110] Zhai L, Liu X, Li T, *et al*. Vacuum and ultrasonic co-assisted electroless copper plating on carbon foams. *Vacuum*, 2015;114:21-25. https://doi.org/10.1016/j.vacuum.2014.12.005

[111] Klett J, Hardy R, Romine E, *et al*. High-thermal-conductivity, mesophase-pitch-derived carbon foams: effect of precursor on structure and properties. *Carbon*, 2000;38(7):953-973. https://doi.org/10.1016/S0008-6223(99)00190-6